Transportation Research Part A 190 (2024) 104260

Contents lists available at ScienceDirect

Transportation Research Part A

journal homepage: www.elsevier.com/locate/tra

Multi-disruption resilient hub location–allocation network design for less-than-truckload logistics

Ahmad Attar [a,b], Chandra Ade Irawan [c,d], Ali Akbar Akbari [e], Shuya Zhong [f,*], Martino Luis [a,b]

[a] Department of Engineering, Faculty of Environment, Science and Economy, University of Exeter, Exeter, United Kingdom
[b] Exeter Digital Enterprise Systems Laboratory, University of Exeter, Exeter, United Kingdom
[c] Nottingham University Business School China, University of Nottingham, Ningbo, China
[d] Nottingham Ningbo China Beacons of Excellence Research and Innovation Institute, Ningbo, China
[e] Department of Industrial Engineering, Islamic Azad University, South Tehran Branch, Tehran, Iran
[f] School of Management, University of Bath, Bath, United Kingdom

ARTICLE INFO

Keywords:
Cargo transportation
Routing policy
Unreliable roads
Hub location problem
Less-than-truckload
Linearization method

ABSTRACT

Less-than-truckload (LTL) logistics presents an interesting and often overlooked practice area of hub location–allocation problems, with its variable discount rates playing a game-changing role. Vulnerability of the roads is another critical factor that has often been neglected when designing hub networks. In this paper, a novel integrated model is designed to solve the LTL hub network design problem, incorporating a practical stepwise discount function. The proposed model is further extended to a reliability-oriented version that can resiliently withstand multiple, simultaneous road disruptions. We use the failure mode and effect analysis (FMEA) technique to encompass the likelihood of experiencing each failure mode, together with the monetary and service-level effects. Coupled with probability theory, it leads to the introduction of a novel closed form for serviceability under multiple concurrent failures. Having such a function enables us to deploy exact optimization methods. Given the natural complexity of the problem, we also present effective linearization approaches. Numerical benchmarks demonstrate the superiority of the novel reliability-oriented approach over the basic version, successfully realizing desired serviceability levels as high as 80%. It also benefits from avoiding unnecessary rerouting, making it even more attractive for policymakers to design efficiently resilient transportation networks, especially if low-range, zero-emission trucks are incorporated.

1. Introduction

The hub-based network structures are widely applied in different areas and industries. These structures are universally adopted by commercial corporations in the fields of transportation, distribution, and telecommunication (Alumur and Kara, 2008; Chen et al., 2010; Adler et al., 2018). In general, these systems are networks of connected centers in which data and material exchange occur solely through a set of preset nodes known as hubs (Martin and Román, 2003; Qu and Weng, 2009; Mohammadi et al., 2013). Compared to a fully interconnected network, such a structure brings about a significant reduction in the number of necessary links within the network (Qu and Weng, 2009). Since the creation of links in a network and the maintenance consume both time and

* Corresponding author.
E-mail addresses: a.attar@exeter.ac.uk (A. Attar), chandra.irawan@nottingham.edu.cn (C.A. Irawan), a_akbari@azad.ac.ir (A.A. Akbari), sz2195@bath.ac.uk (S. Zhong), m.luis@exeter.ac.uk (M. Luis).

https://doi.org/10.1016/j.tra.2024.104260

Available online 19 September 2024

budget, any reductions in the required links result in a more budget-friendly network with faster deployments. This highlights the impact of the hub structure on companies' market share in a competitive delivery market. (Martin and Román, 2003). To benefit from these features, an informed and tactful design of the system is essential to avoid unnecessary routing, both in normal and disruptive situations. The severe consequences of incorrect routing policies span from monetary loss to reputation damage to increments in the network's carbon footprint.

In a hub location problem (HLP) model, cost minimization is the typical objective, and this problem is primarily concerned with two parts of the network design: (i) establishing the hubs, and (ii) assigning the nodes to the hubs (Alumur and Kara, 2008; Farahani et al., 2013; Azizi et al., 2016). One of the most common types of such models is a single-allocation HLP, where each non-hub node in the network is assigned to just one hub, and all incoming and outgoing flows of the node must pass through that single hub (Meier and Clausen, 2018; Contreras and O'Kelly, 2019). Thus the hubs usually have a considerable amount of flow between them, and that is where the economies of scale can lower the transfer cost rates in the network. This concept is commonly considered in the HLP modeling by using a discount factor (α) which only affects the inter-hub transportation (Mohri and Thompson, 2022; Alumur et al., 2021). This factor is dominantly considered as a fixed value, independent to the decisions made by the network administrator (Yang, 2009; Takano and Arai, 2009; Adler et al., 2018; Takebayashi, 2018). However, the widely neglected variable discount factor is an inherent natural property of some real-world systems. Truck shipping and, more specifically, less-than-truckload (LTL) systems are examples of such cases in which the transportation cost per item fluctuates based on the volume of the shipment.

Despite all advantages of the hub network structures, the main drawback of deploying them in the industry is their vulnerability when exposed to any failure or unavailability issues in the hubs themselves or the network links. This can cause over-stacked shipments in one hub that – unless resolved quickly – will epidemically spread to the rest of the hubs, and the entire network will soon be down. For instance, issues like natural disasters, floods, severe weather, employees' strikes, or even terroristic operations can result in a serious disturbance in the transportation and telecommunication networks. In this field of study, the term "unavailability" has generally referred to the unavailability of hubs, while the connecting routes are always considered to be "serviceable". This definition might fit airport hubs or the telecommunications industry, but the LTL transportation network is more likely to encounter a single road blockage while the entire city or hub is still accessible by other routes. Construction operations on roads, restrictions or traffic bans on trucks applied by local authorities on certain roads of a particular city, rockfalls, landslides or snowslides in mountain roads, and serial car accidents, can all block a route to a specific hub while the other routes to the same hub are still up and functioning (Jenelius and Mattsson, 2012; Bíl et al., 2015; Zhang et al., 2020). All of these disruptive situations on roads make it implausible to assume that the hub as a whole is inaccessible, rendering existing models unsuitable for many real systems analogous to LTL.

The significance of this issue is clearly exposed when considering a logistics network like Fig. 1. Despite being a schematic example, this typical hub system considers the major cities in the United Kingdom, which should logically be close to the existing distribution systems in the nation, and can give us a more realistic sense of the issue. In this network, the cities of Norwich and Ipswich, for example, are allocated to a hub in London. In case the links between these cities and their hub get disrupted, they might still be accessible from a nearby hub, say Birmingham, at an extra cost. Considering the hub to be entirely down and allocating all of its cities to a backup hub will be exaggerated because the hub can still serve other cities, e.g., Reading, Oxford, and Brighton. According to our approach, the flow from Aberdeen to Norwich will be delivered through Edinburgh and Birmingham hubs during the disruption of the London-Norwich road. Meanwhile, Aberdeen keeps sending its items to Oxford via the normal route (i.e., Aberdeen-Edinburgh-London-Oxford). Hypothetically, in the optimal solution, the normal route has the lowest cost among all possible routes. So, applying this new approach will save the system from unnecessary usage of the more costly backup hubs or routes.

Neglecting the reliability of the routes significantly affects some key performance indices (KPIs) of the system, such as (i) the overall service level of the network, (ii) the reputation of the transportation company, (iii) the generated revenue, and (iv) the overall contractual penalties paid for unsuccessful deliveries. Unnecessary rerouting to backup hubs, on the other hand, will merely increase the total cost and reduce the competency of the transportation company. Since the network is truck-based, more mileage also means more fuel consumption and higher emissions. If the carbon footprint is considered as a factor in the company's future contracts, this may cause additional threats to its position in the market. With these in mind, in this paper, we develop a realistic and efficiently resilient model for HLP and customize it for the LTL industry so as to minimize the total cost of the network. We also embrace the conceivable scenario in which several roads might be unavailable at the same time, allowing the possibility of having even the backup hubs be inaccessible. Here, we seek to guarantee a minimum level of successful delivery of the flow throughout the system. Considering the contribution of our study to fuel consumption and emissions, it can be considered an endeavor to improve the sustainability of truck-based logistics. Our approach can be an attractive alternative when intermodal road-rail hub workarounds (similar to Mohri and Thompson, 2022) are not implementable. In addition, optimizing the mileage with this method can enhance the practicality of utilizing green trucks running on electricity, fuel cells (hydrogen), liquefied petroleum gas (LPG), or liquefied natural gas (LNG) by reducing the number of required charges per delivery (Siskos and Moysoglou, 2019).

To mitigate the challenge of handling all combinations of road conditions, we utilize a group of advanced techniques from the reliability theory, including failure mode and effect analysis (FMEA) and redundancy allocation. Moreover, hub location–allocation models with reliability are known to be of high degrees of nonlinearity (Barahimi and Vergara, 2020), and the LTL concept (added in this paper) drastically amplifies this characteristic. Therefore, a set of linearization methods is also proposed. The contributions of the paper are outlined in five folds:

- Development of a resilient model by consolidating HLP, LTL, and reliability concepts.

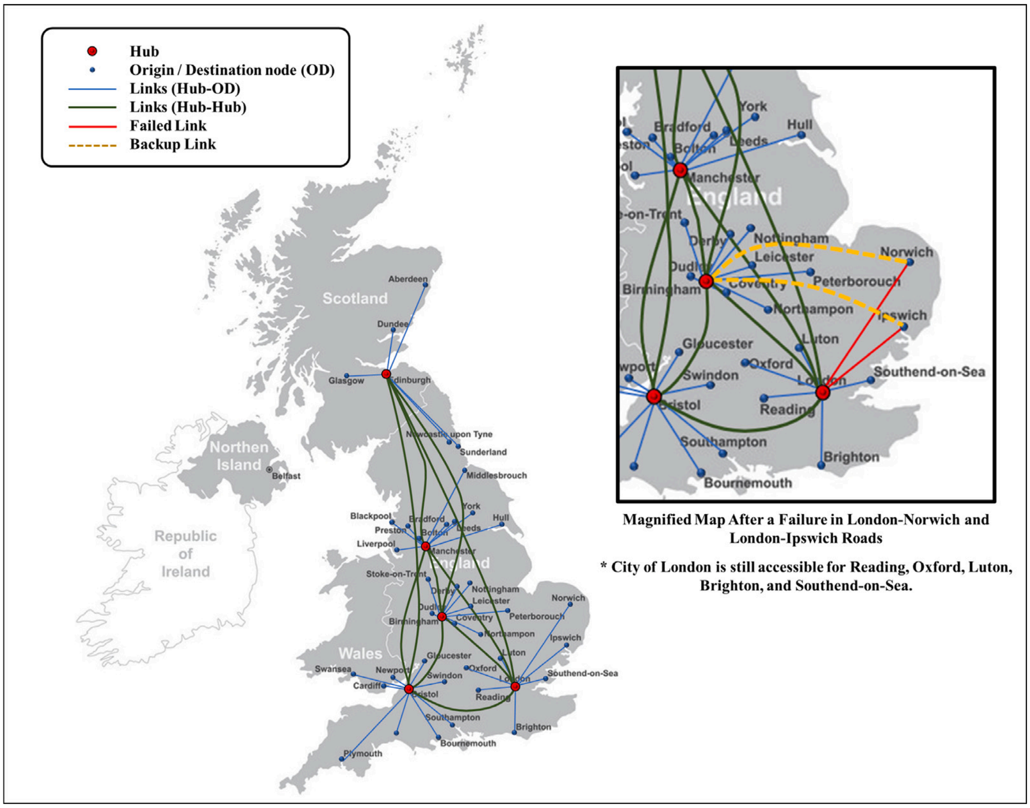

Fig. 1. A schematic illustration of a typical logistics network with single hub allocation in urban delivery of the United Kingdom. Magnified part: our proposed strategy upon multiple failures.

- Consideration of road disruption, and multiple concurrent road blockages or failures in the logistics network.
- Integration of the stepwise discounts with the LTL-HLP.
- Proposing a closed-form function for the serviceability of the system using reliability theory.
- Effective linearization of the complex resilient model.

The rest of the paper is organized as follows: A brief review of the related literature is presented in the following section. In Section 3, we introduce a mathematical model for the simple less-than-truckload hub location model (LTL-HLP) and further develop it into a novel reliability-oriented model. The reliability formulations, along with the linearization methods, are also included in this section. In Section 4.1, the performance of the new model is numerically analyzed under different scenarios. Finally, some concluding remarks and future research directions are presented in Section 5.

2. Literature review

Studies presented by Hakimi (1964) and Toh and Higgins (1985) are among the first works that were accomplished in the HLP area. These were followed by a number of studies by Aykin (1988, 1994, 1995a, 1995b) and Bryan (1998) that developed different models for this field. Alumur and Kara (2008), Farahani et al. (2013), and Azizi et al. (2016) have conducted a thorough review on the diverse types of hub location problems, and concluded that cost minimization is observably the main objective. One of the main characteristics of such problems is the number of hubs to which each mode is allocated. It may appear to be restrictive, but allocating each node to only a single hub benefits from significant consolidation in the inter-hub flow, which has been the focus of numerous studies (e.g., Kim and O'Kelly, 2009; Mohammadi et al., 2013; Meier and Clausen, 2018; Contreras and O'Kelly, 2019; Kara and Tansel, 2000). This assumption implies that in order to deliver goods from one node to another, at least one and at most two hubs are involved (Alumur et al., 2021). This favorable consolidation made the discount factors applied to the inter-hub flow an essential constituent of such transportation systems that lowers the overall cost in accordance with economy-of-scale.

Toh and Higgins (1985), Aykin (1995b), Kara and Tansel (2000), Yang (2009), Takano and Arai (2009), Adler et al. (2018), and Takebayashi (2018) are all among single-allocation HLP studies that successfully considered this factor in their models. However, similar to other studies in this area, they have exclusively considered a fixed α, that makes these models diverge significantly from the truck-based shipping industry. Cunha and Silva (2007) and Lin and Lee (2010) are among the few studies that addressed this issue by proposing variable discount factors. Cunha and Silva (2007) proposed a simple nonlinear model of HLP for the LTL systems in order to minimize the total cost. In this model, the discount factor was assumed to be a load-correlated function. Due to the NP-hard characteristic of the HLP models, the authors proposed a genetic algorithm-based metaheuristic method. Even though addressing the LTL together with HLP was a considerable advantage for this study, their mathematical model was too generic and they did not consider any specific function for their discount factors.

Lin and Lee (2010) considered the LTL hub problem from a competition game perspective for maximizing the total profit of the players in an oligopolistic market. They provided an integral-constrained game theoretic model assuming time-definite less-than-truckload freight services to determine the demand, hub location, and routes. The diagonalization algorithm and Lagrangian relaxation method were used to solve this problem to optimality. More recently, they further studied the time-definite less-than-truckload (LTL) in the delivery industry allowing multiple allocation (Lin and Lee, 2018). Considering the delivery time window, their study explored the behavior of the optimization model for two main scenarios: cost minimization, and profit maximization. Solving their nonlinear capacitated hub model using a Lagrangian relaxation revealed that distinct optimal designs are achieved for these two scenarios. It is worth noting that studies in the LTL industry did not necessarily include hub location–allocation. For example, the very recent research by Tang et al. (2024) viewed this industry from truck-cargo matching and scheduling, and reported impressive benefits for online and on-demand allocation of cargo to the available capacity of trucks. Another attempt is the hybrid hub-and-spoke policy that Hernández et al. (2012) customized for the LTL systems, allowing the customers to subjectively opt out of using the hubs, and consequently, deliver their shipments directly. Undoubtedly, however, such a modified approach suffers from a noticeably limited generality.

As explained in the introduction, a major vulnerability in the hub network is the availability of its components that may cause anything from a local delivery delay to a widespread failure in the system. This challenge stimulated the studies looking at reliability in HLP. As the pioneers in the reliable HLP, Kim and O'Kelly (2009) discussed the reliability of hub networks in the telecommunications industry. Afterwards, this model was further developed for the same industry by Davari et al. (2010) using the fuzzy theory. Both models are mixed integer programming (MIP) with a reliability objective function and considered single-hub allocations. The former, however, used an exact MIP solver (i.e., CPLEX), while the latter solved their model using simulated annealing (SA). An et al. (2015) are among the first researchers who studied the reliable hub location with applications in the logistics area. However, they still assumed that multiple hubs could not fail at the same time. The mixed integer nonlinear programming (MINLP) models provided were solved using a set of Lagrangian relaxation or branch-and-bound algorithms both for single and multiple allocation hub problems.

Azizi et al. (2016) tested another scenario for the hub problems where backups were allocated to the hubs themselves rather than allocating one primary hub and one backup hub to each node. Their model aimed at minimizing the weighted sum of regular and expected transportation costs of the system. It was linearized and solved by using an exact method (CPLEX) for the small instances, and genetic algorithm (GA) for large benchmark problems from the U.S. Civil Aeronautics Board (CAB) and Turkish Postal System (TR) datasets. One of their main findings is that a hierarchical approach to the reliable hub (i.e., the backup assignment problem solved after optimizing the standard hub location–allocation problem) is not as efficient as the concurrent allocation approach. This study was followed by a very similar attempt by Rostami et al. (2018) with the difference of a benders decomposition method in the latter. Azizi and Salhi (2022) investigated a capacitated hub and spoke network problem with disruptions in the hubs and flow-dependent discounts. Unlike other studies that used backups, however, they restricted the system to one backup hub per origin–destination (O–D). In other words, the flow would be forced to pass through only one hub in case of any failures in either the origin or the destination hubs. What makes this type of backup allocation less realistic is that, for example, if only the origin hub is disrupted, not only would the decision maker use a backup hub in place of the failed hub, but they will also deprive the destination node of its normally functioning hub. Azizi and Salhi (2022) also offered a linearized version of the MINLP model, and eventually, for large instances, solved it using reduced variable neighborhood search (RVNS) which did not require a local search.

In most of the studies mentioned above, only half of the flow matrix is considered. Such a symmetrical flow implies that the flow will face the same disruptions when coming back from the destination node towards the origin node (Azizi et al., 2022). Even though this assumption reduces the number of constraints and decision variables significantly, it can be unrealistic in many cases especially if we aim at assigning backup hubs to the nodes. To avoid such limitation, Eydi and Nasiri (2019), Yahyaei et al. (2019), Momayezi et al. (2021), and more recently, Wang et al. (2023) considered the full flow matrix from or to the O–Ds. Successful applications of the described backup assignment can also be found in multiple allocation HLPs (Barahimi and Vergara, 2020; Wang et al., 2023). Moreover, it is worth noting that a hierarchical distribution of flow between multiple assigned hubs is a substitute for the backup assignment strategy. This hierarchical method was introduced recently by Mohammadi et al. (2019) for the multiple allocation HLP where the hub network can fail partially by only passing part of the flow. In this new approach, all assigned hubs may be used even in normal situations and the concept of reserving a backup hub for the disruptions has completely faded. As we are considering road blockage in a truck-based transportation network, this approach does not fit our context. Therefore, we consider a more realistic assumption that when a road is blocked, it will be unavailable for all passing trucks regardless of the amount of load they are carrying.

A summary of the most related hub and LTL problems in the literature is provided in Table 1. To the best of our knowledge, our study is the first one that focuses on a reliability-based HLP in the context of LTL logistics — it consolidates the LTL, HLP, and reliability concepts concurrently. Comparing the studies reported in Table 1 reveals that almost all models in the reliable hub literature are naturally MINLP, and some studies like Barahimi and Vergara (2020) reported very high degrees of nonlinearity. This has led to the introduction of a wide range of linearization methods in the literature, and thus our study involves some linearization reformulations for its novel model. Furthermore, from the reliability perspective, our study can be categorized as a

Table 1
A summary of the related literature in logistics hub location problem and LTL..

Reference	Network design		Disruption area		Asymmetrical flow disruptions	Backups assignment	Hub allocation		Model type[a]	Objective	Solution method			Methodologies and notable assumptions[b]
	LTL	HLP	Hub	Route/ Links			Single	Multi- ple			Exact	Heuristic	Metaheuristic	
Cunha and Silva (2007)	*	*	–	–	N/A	N/A	*		MINLP	Cost			*	Hybrid GA
Lin and Lee (2010)	*	*	–	–	N/A	N/A	*		MINLP	Profit	*			Lagrangian relaxation, Game theory, Diagonalization algorithm, Oligopolistic market
An et al. (2015)		*	*		No	Node	*	*	MINLP	Cost	*			Lagrangian relaxation, Branch-and-bound
Azizi et al. (2016)		*	*		No	Hub	*		MIP	Cost			*	Linearization, CPLEX, GA
Rostami et al. (2018)		*	*		No	Hub	*		MINLP	Cost	*			Benders Decomposition
Lin and Lee (2018)	*	*	–	–	N/A	N/A		*	MINLP	Profit/Cost	*			Lagrangian relaxation, Delivery time-window
Eydi and Nasiri (2019)		*	*		Yes	Node	*		MIP	Reliability		*		Linearization, MA
Yahyaei et al. (2019)		*	*		Yes	Node	*		MIP	Multi	*			Linearization
Mohammadi et al. (2019)		*	*		No	-		*	MIP	Multi		*		Chance constraint, Linearization, SGV-II, Multiple Failures
Barahimi and Vergara (2020)		*	*		No	Node		*	MINLP	Cost	*			Multiple hub failures
Momayezi et al. (2021)		*	*		Yes	Node	*		MIP	Cost		*		Scenario-based, ALNS
Azizi and Salhi (2022)		*	*		Yes	O-D	*		MIP	Cost			*	Flow-dependant, Linearization, RVNS
Wang et al. (2023)		*	*		Yes	Node		*	MIP	Cost	*			Liner Shipping Ports, Benders decomposition
This Paper	*	*		*	**Yes**	**Node**	*		**MIP**	**Cost**	*			**Multiple concurrent failures, FMEA, Linearization, GAMS**

[a] After any linearization attempt (if applicable).
[b] Abbreviations: memetic algorithm (MA), self-adaptive non-dominated sorting genetic algorithm-VNS (SGV-II), adaptive large neighborhood search (ALNS), failure mode and effect analysis (FMEA), general algebraic modeling system (GAMS).

customized instance of the reliability-redundancy allocation problem (RRAP) (Attar et al., 2017, 2023b). That is because, based on the above description of this study, selecting components with higher reliability characteristics (i.e., linked roads) and redundancy (i.e., backup hubs) are considered simultaneously. With reference to the definitions provided by Attar et al. (2023b), our approach is an active-standby strategy as the backup roads may experience failures even if they are not used.

When approaching complex systems with reliability and resiliency factors, other studies typically rely on case-specific estimations or simulation (Barabadi et al., 2014; Attar et al., 2017, 2023a; Shahabi et al., 2022; Tordecilla et al., 2021), which are laborious to implement/use and may not be applied and generalized for other system settings. That is all due to the fact that deriving a closed-form equation for such complex systems is generally very difficult. Nonetheless, it has been demonstrated that a closed-form formula provides a consistent estimator for system indices in a variety of situations (Buccheri et al., 2020; Collin-Dufresne and Harding, 1999; Zhao et al., 2024). As we are targeting decision-makers and policymakers in the logistics field, we aim to introduce an easy-to-use calculation method with a closed-form function to help the implementation of the approach in various logistics settings with minimal effort. Such a function facilitates the use of exact optimization methods, and can also be helpful when studying the sensitivity of the network to fluctuations in its parameters. To achieve this function effectively, we take advantage of probability theory together with the well-known failure mode and effect analysis (FMEA). This method is a systematic process that uses reliability analysis to estimate the performance of the system under known causes of disruptions or risks, which has been applied successfully to various industries such as logistics, food, etc. (Tsai, 2006; Scipioni et al., 2002; Kudláč et al., 2017).

3. Mathematical models

The logistics system designed in this paper integrates three major concepts, namely, hub location–allocation, less-than-truckload, and reliability. In this section, we first present a basic optimization model that integrates HLP in LTL transportation networks (i.e., LTL-HLP). It is followed by the enhanced mathematical model where reliability concepts are injected into the basic model to offer the comprehensive reliability-oriented LTL hub location model (Ro-LTL-HLP).

3.1. Less-than-truckload hub location model (LTL-HLP)

Throughout our modeling phase, we denote C as the set of nodes (cities), with $C = \{1, 2, \dots, n\}$. Let K be the set of candidate hubs. It is common in the HLP literature to assume that this set of locations is identical to the set of nodes, i.e., $K = C$. An $i - j$ flow represents the flow from source node $i \in C$ to destination node $j \in C$, which can be denoted by a 4-tuple (i, k, m, j), where k and m represent the first and the second hubs on the route with $(k, m) \in K$. It is assumed that each node $i \in C$ is allocated to exactly a single hub $k \in K$. Let the traffic volume of the $i - j$ flow be T_{ij}, with C_{ij} be the unit transportation cost between a pair of nodes i and j. When hub $k \in K$ is used, the operating cost of this hub is incurred, denoted by f_k. Due to the economies of scale, there is a discount factor for the inter-hub links ($k - m$ links). In this study, the value of the discount factor depends on the total volume of flow from hub k to hub m (T^{km}). We apply a stepwise function to determine the LTL discounts. Let D be the set of positive discount levels, with $D = \{1, 2, \dots, |D|\}$. Including the cases with zero discount, we define set $E = \{0\} \cup D$ representing the set of all possible discount levels. Parameters α_e and L_e ($e \in E$) are provided to represent the discount factor for the eth level of discount and its minimum required volume of flow between the two hubs, respectively.

The binary variable $X_{ik}, (i, k) \in C$ is the main decision variable of the problem, where $X_{ik} = 1$ when node i is assigned to hub k, and $X_{ik} = 0$ otherwise. The decision on the opening of hub $k \in K$ is represented by $X_{kk}, k \in K$, where $X_{kk} = 1$ if hub k is used, $X_{kk} = 0$ otherwise. Another main binary decision variable is denoted by Y_e^{km}, where $Y_e^{km} = 1$ if the total amount of flow from hub k to hub m qualifies for the eth discount level.

One of the main characteristics of LTL-HLP is its variable discount factors. In this study, this factor is considered as a discrete stepwise function of the total volume of transactions between a pair of hubs. As explained in Section 1, a stepwise approach for the discount factor provides a realistic functionality and is often remarkably close to the common routine in the LTL industry. For each pair of hubs k and m, the applied discount factor (i.e., α^{km}) is calculated by:

$$\alpha^{km} = \begin{cases} \alpha_{|D|}, & \text{if } T^{km} \geq L_{|D|} \\ \alpha_{|D|-1}, & \text{if } L_{|D|} > T^{km} \geq L_{|D|-1} \\ \vdots & \\ \alpha_2, & \text{if } L_3 > T^{km} \geq L_2 \\ \alpha_1, & \text{if } L_2 > T^{km} \geq L_1 \\ \alpha_0 (= 1), & \text{otherwise,} \end{cases} \tag{1}$$

where T^{km} is the total amount of transactions from hub k to hub m. For the eth level of this function, L_e is the minimum amount of flow between the two hubs to qualify for the discount factor α_e ($0 < \alpha_{(e+1)} < \alpha_e < \alpha_{(e-1)} < 1$). As seen in Eq. (1), if the flow between the two hubs does not satisfy the conditions of any discount level, then $\alpha^{km} = 1$ (i.e., no discount is applied to the flow from k to m). Here is where we use set E which includes the no-discount situation ($e = 0$); i.e., $|E| = |D| + 1$. In summary, the mathematical notations used in the model are listed in Table 2.

Our proposed integrated LTL-HLP is designed based on MINLP, which is formulated as follows: **LTL-HLP Model:**

$$\text{Minimize} \quad \sum_{i\in C}\sum_{j\in C}\sum_{\substack{k\in K\\k\neq i}} X_{ik}C_{ik}T_{ij} + \sum_{k\in K}\sum_{m\in K} T^{km}C_{km}\alpha^{km} + \sum_{i\in C}\sum_{j\in C}\sum_{\substack{m\in K\\m\neq j}} X_{jm}C_{mj}T_{ij} + \sum_{k\in K} X_{kk}f_k \tag{2}$$

Table 2
The notations used in the LTL-HLP and Ro-LTL-HLP.

Sets:	
C	Set of nodes (cities), $C = \{1, 2, \dots, n\}$
K	Set of potential hubs, where $K = C$
D	Set of positive discount levels $D = \{1, 2, \dots, \lvert D\rvert\}$
E	$E = \{0\} \cup D$
Parameters:	
T_{ij}	The volume of the flow to be delivered from node i to city j
C_{ij}	Unit cost of transfer from node i to node j
f_k	Cost of using a hub in node k
α_e	The discount factor for the e^{th} level of discounts
L_e	The minimum required amount of flow between a pair of hubs to qualify for the e^{th} level of discounts
Decision variables:	
X_{ik}	$1:$ if node i is assigned to hub k; $0:$ otherwise
X_{kk}	$1:$ if hub k is used; $0:$ otherwise
Y_e^{km}	$1:$ if the total amount of flow from hub k to hub m qualifies for the e^{th} discount level; $0:$ otherwise
Auxiliary variables:	
T^{km}	Total amount of flow from hub k to hub m
T_α^{km}	Auxiliary variable for discounted flow from hub k to hub m
α^{km}	The applied discount factor for the flow between hub k and hub m

Subject to:
$$T^{km} \geq Y_e^{km} L_e, \qquad \forall \{k, m\} \in K, e \in D \tag{3}$$
$$\sum_{e \in E} Y_e^{km} = 1, \qquad \forall \{k, m\} \in K \tag{4}$$
$$X_{ik} \leq X_{kk}, \qquad \forall i \in C, k \in K \tag{5}$$
$$\sum_{k \in K} X_{ik} = 1, \qquad \forall i \in C \tag{6}$$
$$X_{ik} \in \{0, 1\}, \qquad \forall i \in C, k \in K \tag{7}$$
$$Y_e^{km} \in \{0, 1\}, \qquad \forall \{k, m\} \in K, e \in D \tag{8}$$

where:
$$T^{km} = \sum_{i \in C} \sum_{j \in C} X_{ik} X_{jm} T_{ij}, \qquad \forall \{k, m\} \in K \tag{9}$$
$$\alpha^{km} = \sum_{e \in E} \alpha_e Y_e^{km}, \qquad \forall \{k, m\} \in K. \tag{10}$$

The objective function (Eq. (2)) consists of four parts: (i) First part is the costs of transactions from the origin node to the assigned hub, (ii) Second comes the inter-hub flow cost (i.e., travel cost between the origin hub and destination hub), (iii) The third part is the transportation cost of the flow between the destination hub and destination node, and finally (iv) The last part of the function is the hub establishment cost in the selected locations. The first set of constraints (Eq. (3)) determines the discount level for the inter-hub routes based on the total amount of flow between each pair of (k, m) hubs. Here, Y_e^{km} is a Boolean variable that equals 0 unless the flow from hub k to m qualify for the eth discount level. Constraint (4) guarantees that one and only one discount level is applied for each inter-hub road. Assigning each origin or destination node to one hub is done by constraints (5)–(6) that are the common sets of equations for this purpose in the single-allocation HLP literature (check for instance Kim and O'Kelly, 2009; Mohammadi et al., 2013; Meier and Clausen, 2018; Contreras and O'Kelly, 2019; Alumur et al., 2021).

The above integer programming model is currently of degree 3, and that is because of the multiplication of T^{km} and α^{km} in the objective function. So as to lower the degree of the model by one and transform it into a quadratic model, we apply an existing technique from the literature (Kim and O'Kelly, 2009). For this purpose, a new Boolean variable, namely Θ_{ijkm}, is defined that replaces the expression $X_{ik} X_{jm}$ in the above model. Here, Θ_{ijkm} is 1 if the flow from node i to j is assigned to the path $ikmj$ ($i \to k \to m \to j$), 0 otherwise. That is, Θ_{ijkm} becomes 1 if and only if nodes i and j are allocated to hubs k and m. After rewriting Eq. (9), we will have:

$$T^{km} = \sum_{i \in C} \sum_{j \in C} \Theta_{ijkm} T_{ij}, \forall \{k, m\} \in K, \tag{11}$$

and linking the new auxiliary variable to the rest of the model is done through the following constraints:

$$\sum_{m \in K} \Theta_{ijkm} - X_{ik} = 0, \qquad \forall \{i, j\} \in C, k \in K \tag{12}$$
$$\sum_{k \in K} \Theta_{ijkm} - X_{jm} = 0, \qquad \forall \{i, j\} \in C, m \in K. \tag{13}$$

Table 3
The extra notations used in the Ro-LTL-HLP.

Parameters:	
r_{ij}	The reliability of the connecting road between nodes i and j
μ_f	Probability of facing failure mode f
$SF^{kmqh}_{ij,(F,S)}$	Probability of delivering the flow from node i to node j under failure mode F and sub-mode S considering k and m as the main hubs for i, j with q, h as backups
Q^{ij}_{kmqh}	The overall reliability of the flow from i to j with k, m the main hubs and h, q backups
Ω	The desired reliability threshold
Auxiliary variables:	
Z^{qh}_{ijkm}	1 : if nodes i and j are respectively assigned to hubs k and m and backups are q and h; 0 : otherwise.
θ_{ijkm}	Binary variable used in linear reformulation
$W^{qhe,R}_{ijkm}$	Binary variable used in linear reformulation

This has now resulted in a quadratic model for the LTL-HLP that is considered as the base for other models proposed in this paper and will be further developed in the following sections to include other realistic characteristics.

3.2. Reliability-oriented less-than-truckload hub location model (Ro-LTL-HLP)

In general, a normal HLP model tends to select the shortest possible path to transfer the flow between the origin and destination nodes (Alumur and Kara, 2008; Farahani et al., 2013; Contreras and O'Kelly, 2019). In fact, in HLP models, a shorter road (i.e., lower transportation cost) with low reliability is by default preferred to all available roads; even to exceptionally reliable ones. But, as discussed in Section 1, the roads to the selected hubs may encounter failures. The base LTL-HLP model proposed in the previous subsection aims at balancing this desire by considering the discounts that the network can receive by consolidating the inter-hub flows. Nevertheless, that model still has the same reliability weakness.

In this section, we introduce a new model that is built upon the base LTL-HLP and takes into account the unreliability of each road in the network. In the following model, we also add the choice to allocate each node to a backup hub that handles the flow from or to the node in case of any failure in the main hub or its connecting roads. This is all done to find the optimum network design that not only has the minimum total cost but also satisfies the desired minimum service level threshold. The system under study may be described by the following major characteristics and assumptions:

- Each node is allocated to exactly a single main hub, and all incoming (or outgoing) flow to (or from) this node should pass through that hub in normal situations.
- For the case of disturbance, each node may be allocated to at most one backup hub.
- The system incurs a fixed establishment fee when a hub is located in any node.
- Road-blockage applies to all trucks crossing the roads and it is independent of the amount of load carried by the vehicle.
- Roads are failure-prone and have pre-known reliability values.
- Roads of each node are independent in failures.
- Multiple roads may be blocked simultaneously in the network.
- Flow of each origin–destination pair must pass through at least one and at most two hubs.
- The flow matrix can be asymmetrical.
- Road reliability matrix can be asymmetrical, i.e., road form node i to j can be distinct from that of j to i.

The notations used in this new model include the same ones in the previous model (see Table 2), as well as the additions in Table 3.

3.2.1. Reliability functions and route identification

In this subsection, we identify the possible routes in the network, discuss the differences of the current approach with the existing ones, and finally define the reliability functions of the available routes. Fig. 2 presents a schematic view of an LTL hub network with main and backup hubs for two origin nodes (i.e., i and u) and two destinations (i.e., j and w). In this figure, q and h are the backup hubs for i and j, respectively. The flow goes through the route $i-k-m-j$ if all three of the connecting roads are up: Fig. 2.2 (i.e., $i-k$, $k-m$, and $m-j$). In case node i loses access to the road $i-k$ (Fig. 2.3), the flow is redirected to the backup route $i-q$ then depending on the availability of the roads to the destination the least expensive path is chosen, i.e., either $q-m-j$ or $q-h-j$. The most significant difference of the current approach with those HLP models that have considered unreliable hubs (e.g., Kim and O'Kelly, 2009; Davari et al., 2010; An et al., 2015) can be noticed in this figure. The proposed approach lets the network use the hub on some partial failure to deliver the flow from or to other parts of the network. That is, when $i-k$ was blocked and the hub was no longer able to handle the flow from i, node k was not deactivated and it is still used to handle the flow from node u in a completely normal way. If this partial failure happens under an unreliable hub approach, the entire hub is set to be unavailable both nodes i and u must use their backups. Depriving other nodes, here node u, from using their default route will obviously merely increase the total cost and is unrealistic.

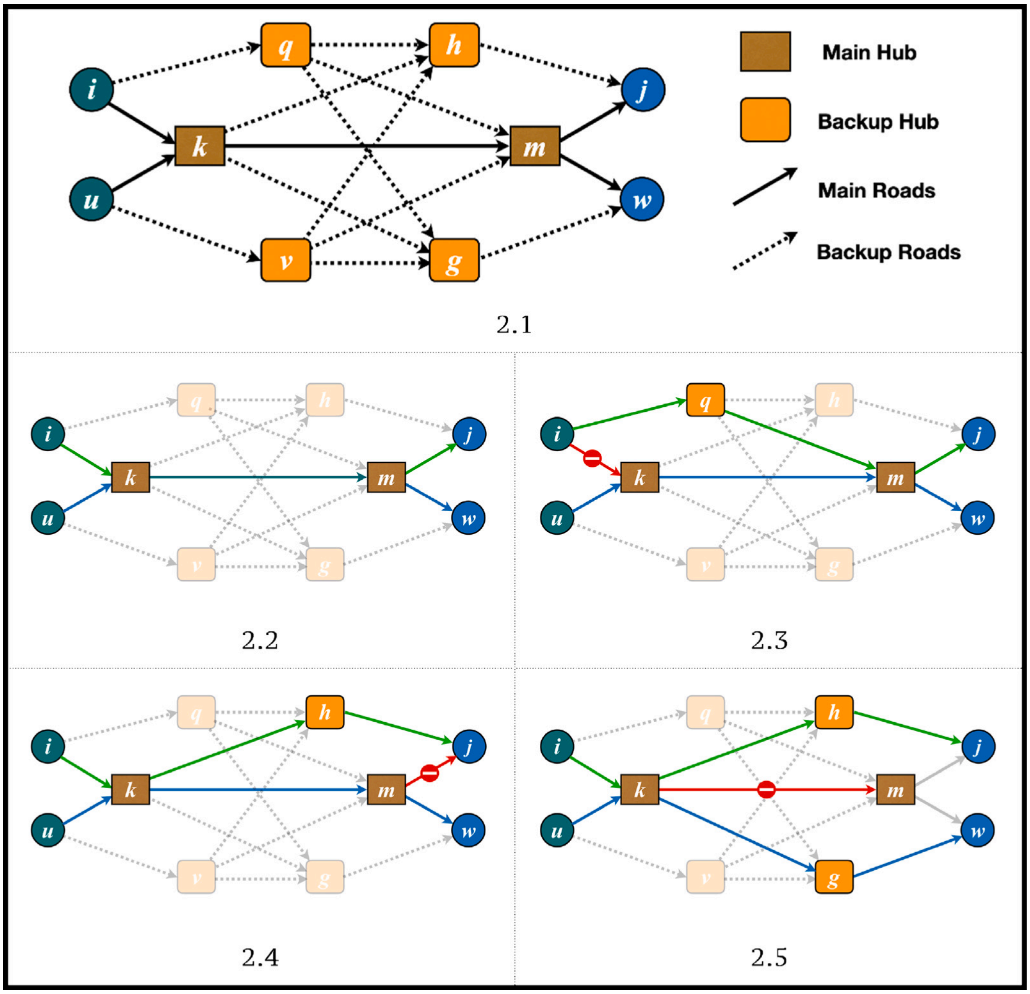

Fig. 2. Schematic structure of a hub network with two origins, two destination nodes, backup hubs, and single disruption.

In order to further explore this network, different graphs are provided in Fig. 3 where two or more links are blocked. We can see that only two situations (Figs. 3.3–3.4) have led to the complete deactivation of hub m, and in the rest, it is still needed. In general, from the above illustrations, we can conclude that the former reliable hub approach is only a special case of the proposed approach where all incoming or outgoing links fail together. Unlike the studies with an unreliable hub approach, the process of including the reliability factor as defined in the current unreliable route approach is not as simple as multiplying a fixed coefficient. Here, reliability theory must be used to derive the reliability of the network. If we reconsider Fig. 2, we can break all possibilities for the flow from i to j into 4 distinct routes:

$R_1 : (i \to k \to m \to j)$ $\qquad$ $R_2 : (i \to k \to h \to j)$

$R_3 : (i \to q \to m \to j)$ $\qquad$ $R_4 : (i \to q \to h \to j)$

By default, the flow passes through R_1 if all three of $i - k$, $k - m$, and $m - j$ routes are up. The probability of such a case is simply the multiplication of the elements in the series (i.e., $r_{ik}r_{km}r_{mj}$). The other routes, however, may be selected on various occasions with regard to the network conditions. Thus, the status of other roads in the network must be taken into account to calculate their probabilities. In LTL networks under study, we define the following logical routing policy rules:

(a) In case the road between one node and its main hub is accessible, the flow from or to this node never gets redirected to its backup hub, i.e., the main hub is always given preference.
(b) In case the connection between the main origin hub and main destination hub is lost, but both origin and destination nodes still have a connection with their main hubs (Fig. 3.2), the backup hub of the origin node will not be used, i.e., the main hub of origin node is given preference.

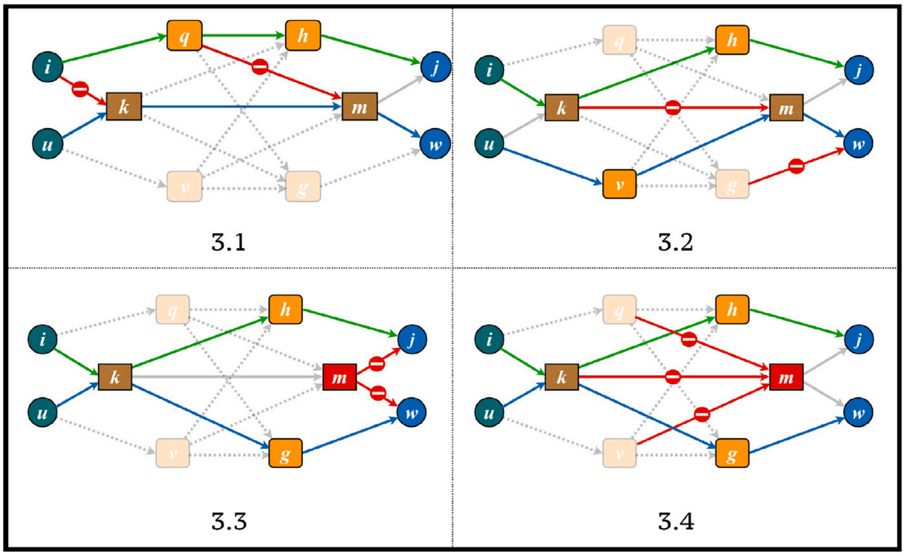

Fig. 3. Schematic view of multiple concurrent failures in different routes in a hub network with backups.

In order to calculate the probability of passing through routes R_2-R_4, we leverage the FMEA techniques from the reliability theory (Carlson, 2014). Among the 2^3 distinct modes that are possible for the elements in the default route (R_1), the route is only up in 1 mode (i.e., mode 0: all three of its elements are up at the same time), and as discussed earlier, calculation of the survival probability of the system under this mode is straight forward (Eq. (14)). Thus, for R_2-R_4, we have 7 different modes of failure. Table 4 includes all possible cases in which the system can successfully deliver the flow from i to j under each possible failure mode and declares the selected route for each case.

This table is meant to disclose the survival probability of the system under each mode of failure. The effect of these modes on the total performance of the network will be discussed in the next subsection while defining new functions for the total flow and cost of the network. Considering the probabilities of R_2-R_4 in each mode (Table 4), the overall probability with which the flow from node i to node j passes through each of the distinct routes of R_1-R_4 are as follows:

$$P^{ij,1}_{kmqh} = SF^{kmqh}_{ij,(0)} = r_{ik} r_{km} r_{mj}, \tag{14}$$

$$P^{ij,2}_{kmqh} = SF^{kmqh}_{ij,(2,1)} + SF^{kmqh}_{ij,(3,1)} + SF^{kmqh}_{ij,(5,1)}, \tag{15}$$

$$P^{ij,3}_{kmqh} = SF^{kmqh}_{ij,(1,1)} + SF^{kmqh}_{ij,(3,2)} + SF^{kmqh}_{ij,(3,3)} + SF^{kmqh}_{ij,(3,4)} + SF^{kmqh}_{ij,(4,1)}, \tag{16}$$

$$P^{ij,4}_{kmqh} = SF^{kmqh}_{ij,(1,2)} + SF^{kmqh}_{ij,(2,2)} + SF^{kmqh}_{ij,(3,5)} + SF^{kmqh}_{ij,(4,2)} + SF^{kmqh}_{ij,(5,2)} + SF^{kmqh}_{ij,(6,1)} + SF^{kmqh}_{ij,(7,1)}, \tag{17}$$

where for each pair (a, b), r_{ab} and r'_{ab} are reliability and unreliability of the road from a to b, respectively. According to reliability theory, reliability and unreliability of ab segment of the network are both probability values which means $0 \leq r_{ab}, r'_{ab} \leq 1$, and they also complement one another; in other words, $r_{ab} + r'_{ab} = 1$ (Navarro, 2022; Attar et al., 2015). The survival function of the system under each mode (SF) is already defined in Table 4. It is noteworthy that all the computations above are predicated on the logical supposition that the main and backup hubs for each node in the system are distinct from one another, i.e., $k \neq q$ and $m \neq h$. That is because it would be completely ambiguous to let a hub serve as a backup upon its own failure. Furthermore, all diagonal elements in the r matrix are equal to 1, which means that the reliability of delivering the goods from each node to itself is always 1 (i.e., practically they are already there). With this in mind, it is straightforward to prove that the above calculations also completely cover the case where the same node, say city k, serves as both origin and destination hubs simultaneously. In such a case, $r_{kk} = 1$ ($r'_{kk} = 0$) and thus the (virtual) link between the origin and destination hubs is completely effectless.

Furthermore, given the fact that the connection of the origin–destination (i, j) is up only in the distinct modes and sub-modes that are discussed above, the overall reliability of the flow from i to j with k, m the main hubs and h, q backups, will be the sum of the survival probability of this connection in each mode:

$$Q^{ij}_{kmqh} = \sum_{(F,S)\in \bar{F}} SF^{kmqh}_{ij,(F,S)}. \tag{18}$$

Here, the set $\bar{F}$ includes all combinations of failure modes (F) and sub-failure modes (S). The formula that we introduced for the first time in Eq. (18) is, in fact, a general closed-form for the serviceability level of each O–D which may be used for other types of analysis in the HLP research area.

Table 4
The specification of each failure mode, their probability, and selected route for keeping the system up.

Mode index	Roads status in failure mode			Probability of facing the failure mode	Sub-mode index	Backup links conditions for flow (i, j) to be up					Selected route	Route notation	Selection reason	Survival probability under each failure mode
	ik	km	mj			iq	qh	hj	qm	kh				
1	D[a]	U[a]	U	$\mu_1 = r'_{ik} r_{km} r_{mj}$	1	U	U				$iqmj$	R_3	Rule (a)	$SF^{kmqh}_{ij,(1,1)} = \mu_1(r_{iq} r_{qm})$
					2	U	U	U	D		$iqhj$	R_4	No other routes	$SF^{kmqh}_{ij,(1,2)} = \mu_1(r_{iq} r_{qh} r_{hj})(r'_{qm})$
2	U	U	D	$\mu_2 = r_{ik} r_{km} r'_{mj}$	1		U		U	$ikhj$	R_2	Rule (a)	$SF^{kmqh}_{ij,(2,1)} =$	$\mu_2(r_{hj} r_{kh})$
					2	U	U	U		D	$iqhj$	R_4	No other routes	$SF^{kmqh}_{ij,(2,2)} = \mu_2(r_{iq} r_{qh} r_{hj})(r'_{kh})$
3	U	D	U	$\mu_3 = r_{ik} r'_{km} r_{mj}$	1			U		U	$ikhj$	R_2	Rule (b)	$SF^{kmqh}_{ij,(3,1)} = \mu_3(r_{hj} r_{kh})$
					2	U		U	U	D	$iqmj$	R_3	Rule (a)	$SF^{kmqh}_{ij,(3,2)} = \mu_3(r_{iq} r_{qm})(r_{hj} r'_{kh})$
					3	U		D	U	U	$iqmj$	R_3	No other routes	$SF^{kmqh}_{ij,(3,3)} = \mu_3(r_{iq} r_{qm})(r'_{hj} r_{kh})$
					4	U		D	U	D	$iqmj$	R_3	No other routes	$SF^{kmqh}_{ij,(3,4)} = \mu_3(r_{iq} r_{qm})(r'_{hj} r'_{kh})$
					5	U	U	U	D	D	$iqhj$	R_4	No other routes	$SF^{kmqh}_{ij,(3,5)} = \mu_3(r_{iq} r_{qh} r_{hj})(r'_{qm} r'_{kh})$
4	D	D	U	$\mu_4 = r'_{ik} r'_{km} r_{mj}$	1	U			U		$iqmj$	R_3	Rule (a)	$SF^{kmqh}_{ij,(4,1)} = \mu_4(r_{iq} r_{qm})$
					2	U	U	U	D		$iqhj$	R_4	No other routes	$SF^{kmqh}_{ij,(4,2)} = \mu_4(r_{iq} r_{qh} r_{hj})(r'_{qm})$
5	U	D	D	$\mu_5 = r_{ik} r'_{km} r'_{mj}$	1			U		U	$ikhj$	R_2	Rule (a)	$SF^{kmqh}_{ij,(5,1)} = \mu_5(r_{hj} r_{kh})$
					2	U	U	U		D	$iqhj$	R_4	No other routes	$SF^{kmqh}_{ij,(5,2)} = \mu_5(r_{iq} r_{qh} r_{hj})(r'_{kh})$
6	D	U	D	$\mu_6 = r'_{ik} r_{km} r'_{mj}$	1	U	U	U			$iqhj$	R_4	No other routes	$SF^{kmqh}_{ij,(6,1)} = \mu_6(r_{iq} r_{qh} r_{hj})$
7	D	D	D	$\mu_7 = r'_{ik} r'_{km} r'_{mj}$	1	U	U	U			$iqhj$	R_4	No other routes	$SF^{kmqh}_{ij,(7,1)} = \mu_7(r_{iq} r_{qh} r_{hj})$

[a] D: down, U: up.

3.2.2. Mathematical model of the Ro-LTL-HLP

Just as we explained in Section 3.1, the discount level of inter-hub transfer is determined based on the total amount of flow that passes from one hub to another. For this reason, the calculation of the total flow between each pair of hubs is a fundamental step in modeling LTL-HLPs. Reliability calculations offered in the last subsection assumed that the origin–destination pair (i, j) both had a main and a backup hub. However, in real networks, we do not want to assign backup hubs (or even to establish ones) without them being necessary for achieving the desired service level. That is, the mathematical model must be free to decide whether or not the node needs a backup hub. Thus, without loss of generality, we add "node 0", which is a dummy node to the network with the following characteristics:

- No flow is assumed from or to this node, i.e., $T_{i0} = T_{0i} = 0, \forall i \in C$.
- No roads are ever available to this virtual node, i.e., $r_{i0} = r_{0i} = 0, \forall i \in C$.
- No fixed establishment cost is assumed for it, i.e., $f_0 = 0$.
- If chosen as a hub, the cost of sending flow to or from it is huge, i.e., $C_{i0} = M, \forall i \in C$.

These specifications guarantee that the new node does not change the definition and conditions of the problem, and is completely lifeless. When a node in the network chooses this dummy node as the backup hub, it will neither get any benefit of this choice, nor cost the network — exactly equivalent to choosing no backups. Accordingly, two new sets, namely, K' and C' are defined that include this dummy node together with all existing cities from sets C and K, respectively (i.e., $C' = \{0\} \cup C$ and $K' = \{0\} \cup K$). The expected value of T^{km} for this novel model (after including the dummy node) is derived by Eq. (19):

$$T^{km} = \sum_{i\in C}\sum_{j\in C} T_i j \times \sum_{q\in K'}\sum_{h\in K'} [Z^{qh}_{ijkm}(P^{ij,1}_{kmqh}) + Z^{qm}_{ijkh}(P^{ij,2}_{khqm}) + Z^{kh}_{ijqm}(P^{ij,3}_{qmkh}) + Z^{km}_{ijqh}(P^{ij,4}_{qhkm})]. \tag{19}$$

Here, $Z^{qh}_{ijkm} = X_{ik}X_{jm}X^B_{iq}X^B_{jh}$, and the new variable X^B_{ia} is a binary decision variable which equals 1 only if node a is the backup hub of node i. The first term in the square brackets reflects the situation where both k and m are the main hubs. The 2[nd] and 3[rd] parts are related to cases in which only one of them is a backup hub; and in the last part, k and m are both backup hubs. The other important aspect of the new model is its cost function. Eq. (20) presents the new estimated cost function of the network with respect to the reliability of the routes.

$$\text{Cost} = \sum_{i\in C}\sum_{j\in C} T_{ij} \times \sum_{\substack{k\in K\\ k\neq i}}\sum_{\substack{m\in K\\ m\neq j}}\sum_{\substack{q\in K'\\ q\neq i}}\sum_{\substack{h\in K'\\ h\neq j}} Z^{qh}_{ijkm}\Phi + \sum_{k\in K}\sum_{m\in K} T^{km}C_{km}\alpha^{km} + \sum_{k\in K} X_{kk}f_k, \tag{20}$$

where $\Phi = P^{ij,1}_{kmqh}(C_i k + C_m j) + P^{ij,2}_{kmqh}(C_{ik} + C_{hj}) + P^{ij,3}_{kmqh}(C_{iq} + C_{mj}) + P^{ij,4}_{kmqh}(C_{iq} + C_{hj})$ and the definitions in Eqs. (10) and (19) are used for calculating α^{km} and T^{km}, respectively. Eventually, the mathematical model for the Ro-LTL-HLP can be provided as below:

Ro-LTL-HLP Model:

$$\text{Minimize} \quad \text{Cost} \tag{21}$$

$$\text{Subject to:} \quad T^{km} \geq Y^{km}_e L_e, \qquad \forall \{k, m\} \in K, e \in D \tag{22}$$

$$\sum_{e\in E} Y^{km}_e = 1, \qquad \forall \{k, m\} \in K \tag{23}$$

$$X_{ik} + X^B_{ik} \leq X_{kk}, \qquad \forall i \in C', k \in K' \tag{24}$$

$$\sum_{k\in K} X_{ik} = 1, \qquad \forall i \in C' \tag{25}$$

$$\sum_{\substack{k\in K'\\ (k\neq i)}} X^B_{ik} = 1, \qquad \forall i \in C' \tag{26}$$

$$\sum_{k\in K}\sum_{m\in K}\sum_{q\in K'}\sum_{h\in K'} Z^{ij}_{kmqh}Q^{ij}_{kmqh} \geq \Omega, \qquad \forall \{i, j\} \in C', j \neq i \tag{27}$$

$$X_{ik} \in \{0, 1\}, \qquad \forall i \in C', k \in K' \tag{28}$$

$$X^B_{ik} \in \{0, 1\}, \qquad \forall i \in C', k \in K' \tag{29}$$

$$Y^{km}_e \in \{0, 1\}, \qquad \forall \{k, m\} \in K', e \in E. \tag{30}$$

The above model assigns each node to one main and one backup hub (Eqs. (25)–(26)) and ensures that the hub is established before assignment (Eq. (24)). Choosing the main hub as a backup is not logical. It would also contradict the underlying assumptions of our reliability calculations in Section 3.2.1. Thus, constraint (24) is defined in such a way that along with its mentioned role in hub establishments, prevents the model from a duplicate assignment. Note that, doing the summation in constraint (25) on set K (i.e., $k = 1, 2, 3, \ldots, n$), keeps the model from choosing node 0 as the main hub. In an effort to maintain a minimum service level of Ω for the flow between origin and destination nodes, inequality (27) is added to the model in which Q is the overall reliability of the flow and has already been defined in Section 3.2.1.

Earlier in Table 4, we used the FMEA concept for our reliability formulations. If we reconsider constraint (22) along with (19), we can see that the modes defined in that table directly affect the ability of the entire LTL network to take advantage of the economies of scale on different links. In fact, unreliable roads will have lower values of expected flow passing through them and the expected received discounts for the passing flow will be downgraded as such. On the other hand, the total cost function in Eq. (20) demonstrates two effects that the modes can have on the system: (i) it considers the reliability of the roads while calculating the inter-hub transfer cost, which in fact is the effect of allocated discount level and total flow, and (ii) in the first part of the cost function, we have the direct effect of the survival probability of the routes in the flow between the hubs and the origin or destination node. Another effect of the defined failure modes is the overall service level of the network, which is controlled using constraint (27). The service level can also be interpreted as the reputation of the company or even as a positive leverage that will be used in negotiations for future contracts.

3.2.3. Linear reformulation for the Ro-LTL-HLP

Substituting T^{km} and α^{km} in the cost function of the Ro-LTL-HLP Model (from Eqs. (10) and (19), respectively) results in a mathematical model of degree five. In provision for its transformation to a quadratic model (similar to the LTL-HLP Model), we need to reduce the degree of the new T^{km} by 3. In the linearization literature, various techniques have been introduced for linearizing the product of several binary variables. The general method offered by Ghezavati and Saidi-Mehrabad (2011) was shown to be much more efficient in comparison with the other techniques in the literature, including the one provided by Chang and Chang (2000). The main advantage of Ghezavati and Saidi-Mehrabad's method is its significantly reduced number of auxiliary constraints that should be added to the model for linearization purposes. In this study, we present a customized version of their method in which only two new sets of constraints are required.

Linearization Method 1. In place of the product style definition for Z, the proposed method links this variable to the hub allocation variables by using the following sets of constraints:

$$Z_{ijkm}^{qh} \geq \left(\frac{X_{ik} + X_{jm} + X_{iq}^B + X_{jh}^B}{4} - \frac{3}{4} \right), \qquad \forall \{i,j\} \in C', \{q,h\} \in K', \{k,m\} \in K \tag{31}$$

$$Z_{ijkm}^{qh} \leq \left(\frac{X_{ik} + X_{jm} + X_{iq}^B + X_{jh}^B}{4} \right), \qquad \forall \{i,j\} \in C', \{q,h\} \in K', \{k,m\} \in K \tag{32}$$

$$Z_{ijkm}^{qh} \in \{0,1\}, \qquad \forall \{i,j\} \in C', \{q,h\} \in K', \{k,m\} \in K. \tag{33}$$

Proof. ***(a)*** if for a unique set of (i,j,k,m,q,h), we have $X_{ik} = X_{jm} = X_{iq}^B = X_{jh}^B = 1$, then the above two constraints become $Z_{ijkm}^{qh} \geq 1/4$, and $Z_{ijkm}^{qh} \leq 1$; consequently, the binary variable Z_{ijkm}^{qh} equals 1. ***(b)*** otherwise, if at least one of the X variables in the summation is 0, then the constraints become $Z_{ijkm}^{qh} \geq e(-3/4 \leq e \leq 0)$, and $Z_{ijkm}^{qh} \leq 3/4$; then with Z_{ijkm}^{qh} being a $0-1$ variable, it gets 0. □

It is notable that this method is completely general and is not dependent on the other constraints for it to be correct. This makes it fully adaptable to any other problems with functions in the form of binary product. With the above method, we have a linear definition for T^{km}. This means that the model is linear except for the objective cost function (Eq. (20)) which is now quadratic. In the following method, we take another step forward in order to achieve a fully linearized version of the Ro-LTL-HLP Model by trying to linearize the second part of the cost function, i.e., $\sum_{k\in K}\sum_{m\in K} T^{km} C_{km} \alpha^{km}$ (the only remaining nonlinear part of the model).

Linearization Method 2. Here, we define the auxiliary variable $W_{ijkm}^{qhe,R}$ in which $R = \{1,2,\ldots,4\}$ and for the 4 possible R values, we have:

$$\begin{cases} Y_e^{km} Z_{ijkm}^{qh} & \to W_{ijkm}^{qhe,1} \\ Y_e^{km} Z_{ijqm}^{kh} & \to W_{ijkm}^{qhe,2} \\ Y_e^{km} Z_{ijkh}^{qm} & \to W_{ijkm}^{qhe,3} \\ Y_e^{km} Z_{ijqh}^{km} & \to W_{ijkm}^{qhe,4} \end{cases}, \qquad W_{ijkm}^{qhe,R} \in \{0,1\}. \tag{34}$$

In order for these variables to be linked to their new substitute, we can use Ghezavati and Saidi-Mehrabad's method just as we did in Method 1, which would add $8n^4(n+1)^2|E|$ new auxiliary constraints to our model. Since number of constraints is substantial for the solution time of linear models, we propose the following sets of constraints that linearize the above relations and only require a fraction of this number of constraints to be added:

$$\sum_{q\in K'}\sum_{h\in K'} W_{ijkm}^{qhe,R} \leq Y_e^{km}, \qquad \forall \{i,j\} \in C', \{k,m\} \in K, e \in E, R \in \{1,2,3,4\} \tag{35}$$

$$\sum_{e\in E} W_{ijkm}^{qhe,1} = Z_{ijkm}^{qh}, \qquad \forall \{i,j\} \in C', \{q,h\} \in K', \{k,m\} \in K \tag{36}$$

$$\sum_{e\in E} W_{ijkm}^{qhe,2} = Z_{ijkh}^{qm}, \qquad \forall \{i,j\} \in C', \{q,h\} \in K', \{k,m\} \in K \tag{37}$$

$$\sum_{e\in E} W_{ijkm}^{qhe,3} = Z_{ijqm}^{kh}, \qquad \forall \{i,j\} \in C', \{q,h\} \in K', \{k,m\} \in K \tag{38}$$

$$\sum_{e\in E} W_{ijkm}^{qhe,4} = Z_{ijqh}^{km}, \qquad \forall \{i,j\} \in C', \{q,h\} \in K', \{k,m\} \in K. \tag{39}$$

The total number of constraints in Eqs. (35)–(39) is only $4n^4((n+1)^2+|E|)$, which for realistic networks with n significantly greater than $|E|$, is $1/2|E|$ of the number of constraints required by the above-mentioned method of Ghezavati and Saidi-Mehrabad (2011).

Proof. *Step One:* First, we check whether the new variables get zeroes when they should.

- **(i)** For $k=k'$, $m=m'$, and $e=e'$, if $Y_e^{km}=0$, then given the binary nature of W, the set of constraints in (35) forces $W_{ijkm}^{qhe,R}=0$ for all i,j,q,h,R values. Note that, from Eq. (23), we know that there exists one and only one Y that equals 1 for each pair k,m (which of course has an e value other than e'); this means that Eqs. (36)–(39) will still hold even after zeros are forced for the above variables.
- **(ii)** On the other hand, for an arbitrary pair of i,j, if $Z_{ijkm}^{qh}=0$ ($k=k'$, $m=m'$, $q=q'$, and $h=h'$) : then Eq. (36) sets all $W_{ijkm}^{qhe,1}$ variables to 0 regardless of the Y values. A similar reasoning easily proves the respective relation between $W_{ijkm}^{qhe,2}$, $W_{ijkm}^{qhe,3}$, $W_{ijkm}^{qhe,4}$ values and the corresponding Z variables.

From **(i)** and **(ii)**, we can conclude that each W is forced to get 0 if a 0 is set for at least one of the corresponding Y or Z variables, i.e.,

$$\{Y_e^{km}=0 \quad \vee \quad Z_{ij}^{R}=0\} \equiv \{W_{ijkm}^{qhe,R}=0\}, \tag{40}$$

where $\vee$ is the inclusive disjunction symbol and Z_{ij}^{R} denotes Z_{ijkm}^{qh}, Z_{ijkh}^{qm}, Z_{ijqm}^{kh}, Z_{ijqh}^{km} for R values 1–4, respectively.

Step Two: What we have left for the proof to be complete is only showing how the right variable gets 1. For this purpose, let i,j be an arbitrary pair of nodes, if both $Y_e^{km}=1$ and $Z_{ijkm}^{qh}=1$ ($k=k'$, $m=m'$, $q=q'$, $h=h'$, and $e=e'$) then Eqs. (35) and (36) can be rewritten as $\sum_{q\in K'}\sum_{h\in K'}W_{ijkm}^{qhe,R}\le 1$ and $\sum_{e\in E}W_{ijkm}^{qhe,1}=1$, respectively. We also know that only one Z for each pair of i,j is 1 and this has already been guaranteed using Eqs. (24)–(26) and (31)–(33). Thus, $Z_{ijkm}^{qh}=0$ if $k\neq k'$ OR $m\neq m'$ OR $q\neq q'$ OR $h\neq h'$; that is $Z_{ijqm}^{kh}=Z_{ijkh}^{qm}=Z_{ijqh}^{km}=0$. Consequently, from the first step, we have $W_{ijkm}^{qhe,2}=W_{ijkm}^{qhe,3}=W_{ijkm}^{qhe,4}=0$ for all k,m,q,h,e values other than k',m',q',h',e'.

Additionally, for $R=1$, Eq. (23) ensures that only one Y is set to 1 for each pair (k,m). Consequently, as we showed earlier, all $W_{ijkm}^{qhe,R}$ variables (including all $W_{ijkm}^{qhe,1}$) are forced to 0 by constraint set (35) except for the ones with $e=e'$. This means that Eq. (36) can be further simplified as $W_{ijkm}^{qhe,1}=1$ for $k=k'$, $m=m'$, $q=q'$, $h=h'$, only when $e=e'$. Proofing this relation for other R values is straightforward. In turn, this step of the proof can be summarized as:

$$\{Y_e^{km}=1 \quad \wedge \quad Z_{ij}^{R}=1\} \equiv \{W_{ijkm}^{qhe,R}=1\}, \tag{41}$$

where $\wedge$ is the logical conjunction symbol. By considering Eqs. (40)–(41), the proof is complete. □

For future reproduction of this linearization method, it should be noted that Method 2 (unlike Method 1) is problem-specific and cannot be used for other problems unless other constraints that were used in the proof also hold; i.e., already exist in the new models or should be added as well. By substituting $W_{ijkm}^{qhe,R}$ in Eq. (20), it can be reformulated in the following linear form which results in a fully linearized model:

$$\text{Cost}=\sum_{i\in C}\sum_{j\in C}T_{ij}\times\sum_{\substack{k\in K\\k\neq i}}\sum_{\substack{m\in K\\m\neq j}}\sum_{\substack{q\in K'\\q\neq i}}\sum_{\substack{h\in K'\\h\neq j}}Z_{ijkm}^{qh}\Phi+\sum_{k\in K}\sum_{m\in K}T_{\alpha}^{km}C_{km}+\sum_{k\in K}X_{kk}f_k, \tag{42}$$

where Φ is just as defined for Eq. (20) and the auxiliary variable T_{α}^{km} is calculated by:

$$T_{\alpha}^{km}=\sum_{i\in C}\sum_{j\in C}T_{ij}\times\sum_{q\in K'}\sum_{h\in K'}\sum_{e\in E}\alpha_e[W_{ijkm}^{qhe,1}(P_{kmqh}^{ij,1})+W_{ijkm}^{qhe,2}(P_{khqm}^{ij,2})+W_{ijkm}^{qhe,3}(P_{qmkh}^{ij,3})+W_{ijkm}^{qhe,4}(P_{qhkm}^{ij,4})].$$

It is important to note that, as demonstrated by the mathematical proofs of our linearization methods, the solution space of the linearized version remains precisely the same as the original Ro-LTL-HLP. As a result, the fully linearized model benefits from an exact solution identical to that of the non-linear version of Ro-LTL-HLP.

4. Computational experiments and result analysis

4.1. Evaluation on the proposed model

In this section, a set of numerical experiments is designed to help demonstrate the functionality of the proposed Ro-LTL-HLP model under different possible scenarios. For this purpose, we assume an LTL network with n nodes and 2 positive discount levels ($|E|=3$) for which the basic specifications are given in Table 5. Some of these distributions are selected in accordance with the numerical cases explored by Niknamfar et al. (2017).

With the aim of performing the analysis of this section, the proposed mathematical model is coded in the general algebraic modeling system (GAMS) 32.2, and it is examined against 42 configurations in six distinct scenario groups. Fig. 4 graphically illustrates the configuration of these scenario groups (hereinafter scenarios) and their corresponding sub-scenarios. The first three scenarios are defined with $\sigma_{\alpha}=0$ for which the results of our model are presented in Table 6. These are mainly for analyzing the

Table 5
Parameter settings for the LTL network under study.

Parameter	Value
r_{ij}	Uniform(0.6, 0.8)
T_{ij}	Uniform(500, 700)
C_{ij}	Uniform(10, 20)
f_k	Uniform($100\sigma_F$, $150\sigma_F$)
$L_e[\alpha_e]$	$0[1.0], 800[0.9-\sigma_\alpha], 1000[0.8-\sigma_\alpha]$

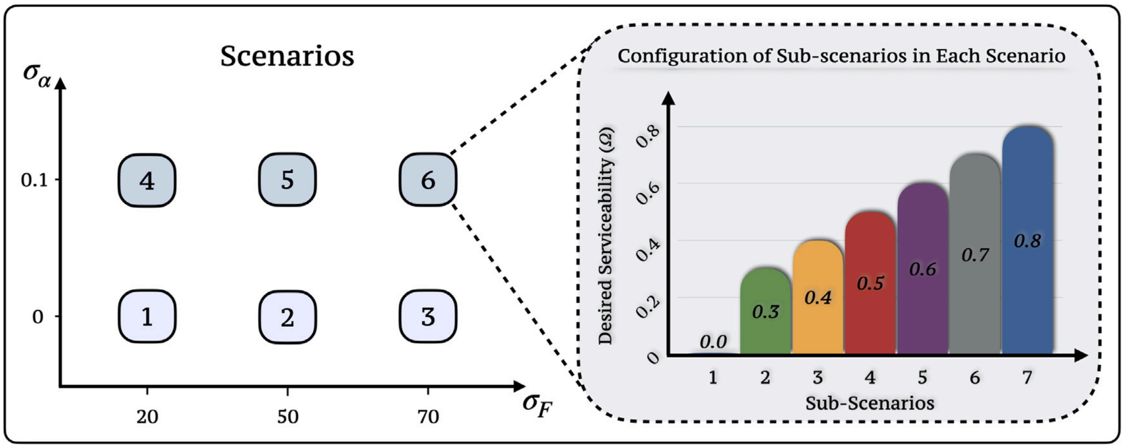

Fig. 4. Definition of scenarios and sub-scenarios in the performed experiments.

Table 6
Optimal design for Scenarios 1-3.

	Ω	Hubs	# Nodes with backups	# Hubs as backup	Flow reliability			Total discount	Cost		
					Min	Mean	Max		Fixed	Variable	Total
Scenario 1 ($\sigma_F = 20, \sigma_\alpha = 0$)	–	1,2,3,4	–	–	0.671	0.740	0.796	–	9049.27	83897.28	92946.55
	0.3	1,2,3,4	–	–	0.671	0.740	0.796	–	9049.27	83897.28	92946.55
	0.4	1,2,3,4	–	–	0.671	0.740	0.796	–	9049.27	83897.28	92946.55
	0.5	1,2,3,4	–	–	0.671	0.740	0.796	–	9049.27	83897.28	92946.55
	0.6	1,2,3,4	–	–	0.671	0.740	0.796	–	9049.27	83897.28	92946.55
	0.7	1,2,3,4	2	1	0.700	0.881	0.961	–	9049.27	107119.69	116168.97
	0.8	1,2,3,4	3	3	0.846	0.925	0.979	–	9049.27	115011.13	124060.40
Scenario 2 ($\sigma_F = 50, \sigma_\alpha = 0$)	–	2 , 4	–	–	0.352	0.590	0.781	7372.73	10444.49	90281.35	100725.84
	0.3	2 , 4	–	–	0.352	0.590	0.781	7372.73	10444.49	90281.35	100725.84
	0.4	2 , 4	–	–	0.509	0.627	0.781	6188.77	10444.49	94013.56	104458.05
	0.5	2 , 4	–	–	0.509	0.627	0.781	6188.77	10444.49	94013.56	104458.05
	0.6	1,2,3,4	–	–	0.671	0.740	0.796	–	22623.18	83897.28	106520.46
	0.7	1,2,3,4	2	1	0.700	0.881	0.961	–	22623.18	107119.69	129742.87
	0.8	1,2,3,4	3	3	0.846	0.925	0.979	–	22623.18	115011.13	137634.30
Scenario 3 ($\sigma_F = 70, \sigma_\alpha = 0$)	–	2 , 4	–	–	0.352	0.589	0.781	7372.73	14622.29	90281.35	104903.64
	0.3	2 , 4	–	–	0.352	0.589	0.781	7372.73	14622.29	90281.35	104903.64
	0.4	2	–	–	0.509	0.627	0.781	–	7254.69	100202.32	107457.01
	0.5	2	–	–	0.509	0.627	0.781	–	7254.69	100202.32	107457.01
	0.6	1,2,3,4	–	–	0.671	0.740	0.796	–	31672.45	83897.28	115569.73
	0.7	1,2,3,4	2	1	0.700	0.881	0.961	–	31672.45	107119.69	138792.14
	0.8	1,2,3,4	3	3	0.846	0.925	0.979	–	31672.45	115011.13	146683.57

sensitivity of the optimal solution of the Ro-LTL-HLP model to the desired reliability threshold under different distribution properties for the fixed establishment cost.

For each scenario, Table 6 includes the index of nodes chosen as hubs, number of nodes that were assigned a backup hub, number of nodes that have dual functions (i.e., both as primary and backup), min, max, and average level of the reliability of the flow between each origin–destination pair, total discount achieved by the network, and details on the cost function values. Each section of this table comprises 6 rows for a range of Ω values, and one row for the case where no restriction is imposed on the reliability (i.e., the traditional approach with no serviceability mandates). The time elapsed for solving most of these scenarios is less than 30 s

Table 7
Optimal design for Scenarios 4-6.

	Ω	Hubs	# Nodes with backups	# Hubs as backup	Flow reliability			Total discount	Cost		
					Min	Mean	Max		Fixed	Variable	Total
Scenario 4 ($\sigma_F = 20, \sigma_\alpha = 0.1$)	–	2 , 4	–	–	0.352	0.590	0.781	11059.10	4177.80	86594.98	90772.78
	0.3	2 , 4	–	–	0.352	0.590	0.781	11059.10	4177.80	86594.98	90772.78
	0.4	1,2,3	–	–	0.517	0.670	0.796	10556.06	6944.24	85447.08	92391.32
	0.5	1,2,3	–	–	0.517	0.670	0.796	10556.06	6944.24	85447.08	92391.32
	0.6	1,2,3,4	–	–	0.671	0.740	0.796	–	9049.27	83897.28	92946.55
	0.7	1,2,3,4	2	1	0.700	0.881	0.961	5213.02	9049.27	106440.58	115489.85
	0.8	1,2,3,4	3	3	0.846	0.925	0.979	2049.24	9049.27	114711.48	123760.75
Scenario 5 ($\sigma_F = 50, \sigma_\alpha = 0.1$)	–	2 , 4	–	–	0.352	0.590	0.781	11059.10	10444.49	86594.98	97039.47
	0.3	2 , 4	–	–	0.352	0.590	0.781	11059.10	10444.49	86594.98	97039.47
	0.4	1 , 2	–	–	0.404	0.623	0.796	13233.23	10493.98	90224.66	100718.64
	0.5	2 , 3	–	–	0.509	0.627	0.781	10908.96	12048.55	89293.37	101341.91
	0.6	1,2,3,4	–	–	0.671	0.740	0.796	–	22623.18	83897.28	106520.46
	0.7	1,2,3,4	2	1	0.700	0.881	0.961	5213.02	22623.18	106440.58	129063.75
	0.8	1,2,3	3	3	0.832	0.900	0.98	17620.39	17360.60	119375.80	136736.41
Scenario 6 ($\sigma_F = 70, \sigma_\alpha = 0.1$)	–	2 , 4	–	–	0.352	0.590	0.781	11059.10	14622.29	86594.98	101217.27
	0.3	2 , 4	–	–	0.352	0.590	0.781	11059.10	14622.29	86594.98	101217.27
	0.4	1 , 2	–	–	0.404	0.623	0.796	13233.23	14691.57	90224.66	104916.23
	0.5	2 , 4	–	–	0.509	0.627	0.781	9283.15	14622.29	90919.17	105541.46
	0.6	1,2,3,4	–	–	0.671	0.740	0.796	–	31672.45	83897.28	115569.73
	0.7	1,2,3	3	2	0.700	0.856	0.946	13207.697	24304.85	113255.65	137560.50
	0.8	1,2,3	3	3	0.832	0.900	0.98	17620.39	24304.85	119375.80	143680.65

considering our proposed linearization methods using CPLEX solver. In order to test the effectiveness of our proposed linearization approach, we attempted to use a well-known nonlinear solver (i.e., BARON) to solve the same scenarios on the initial (nonlinear) version of Ro-LTL-HLP model. For all scenarios, no feasible solution was found by BARON after the default maximum allowable time elapsed (1000 s). Time-wise, this observation by itself attests to the significant effectiveness of the introduced linearization techniques. Speed superiority together with other significant features of the proposed linearization are further demonstrated in the detailed comparative results of Appendix considering few alternative exact and metaheuristic benchmark techniques.

According to the results provided in Table 6, it is observed that when the fixed cost is low (Scenario 1) the model tends to establish as many hubs as possible and it never consolidated the flow (i.e., no discounts). By looking at the reliability columns, however, we clearly see that the model has completely been successful in complying with the desired threshold and all reliability indices have increased accordingly in the last two rows of this scenario by assigning backup hubs to the nodes. It is also noticed that even in the base condition with no reliability threshold, the optimal solution is exemplary and its reliability is around 70% for all origin–destinations in the network.

But, as we increase the fixed establishment cost in Scenario 2, the minimum reliability falls to 35.2% for the base case, with the average being 59%. It was predictable that the base optimal solution will be optimal for other cases until Ω becomes greater than 35%. Unlike the earlier scenario, the optimal design only has two hubs and has acquired a significant amount of discount for its traffic consolidations. In $\Omega = 0.6$ (which seems to be the knee point in all scenarios), the base combination of hubs no longer is capable of satisfying the desired service level and the model moves towards more hub establishments. For a reliability threshold of 70% and higher, the model uses the backup assignments, and the higher the reliability threshold, the more backups are required.

When we increase the average establishment cost of the system in Scenario 3, the model was expected to opt for a smaller number of hubs. This is what happened in $\Omega = 0.4$ and 0.5, where the model preferred to establish only one hub (i.e., node 2) and successfully satisfied the desired Ω even without backup assignments. It is notable that in this case, the total discount is zero. That is because the origin and destination hubs are both the same, and practically there is no inter-hub traffic to charge a fee on. But we see that the fixed cost in the new network is less than half of the base solution which by itself has resulted in about 7300 unit cost and it is almost the same as the amount we have for the discount in the base case. Nevertheless, even with the zero inter-hub transfer cost that this design benefits from, the one-hub design has a higher variable cost. The reason behind this must be the higher transfer costs from or to node 2 in the random input data. This can also explain the reason why the one-hub design has been avoided in the first two cases. Altogether it shows that the model has sufficiently done a trade-off between the fixed cost and the variable cost, and the final decision was made based on the total cost of the design. Table 7 provides the optimal solution for Scenarios 4–6 and includes the same indices as we had for the first three scenarios.

Here, we intend to analyze the sensitivity of the model to changes in the discount factors of the LTL system. To avoid any bias in the outcome of our analyses, L_e values are fixed to the same amounts we had in the previous scenarios. Comparing these scenarios with their counterparts in Table 6 shows that the model has completely appreciated the decrement in the discount factor and has gone towards more consolidations, even from the very first case. For a more thorough comparison of the scenario sets, we visualize the data presented in Tables 6–7 via three sets of charts in Figs. 5–7. The amount of fixed and variable costs that constitute the total cost in the six scenarios are plotted in Fig. 5 under an assortment of levels for the desired reliability. This figure suggests that

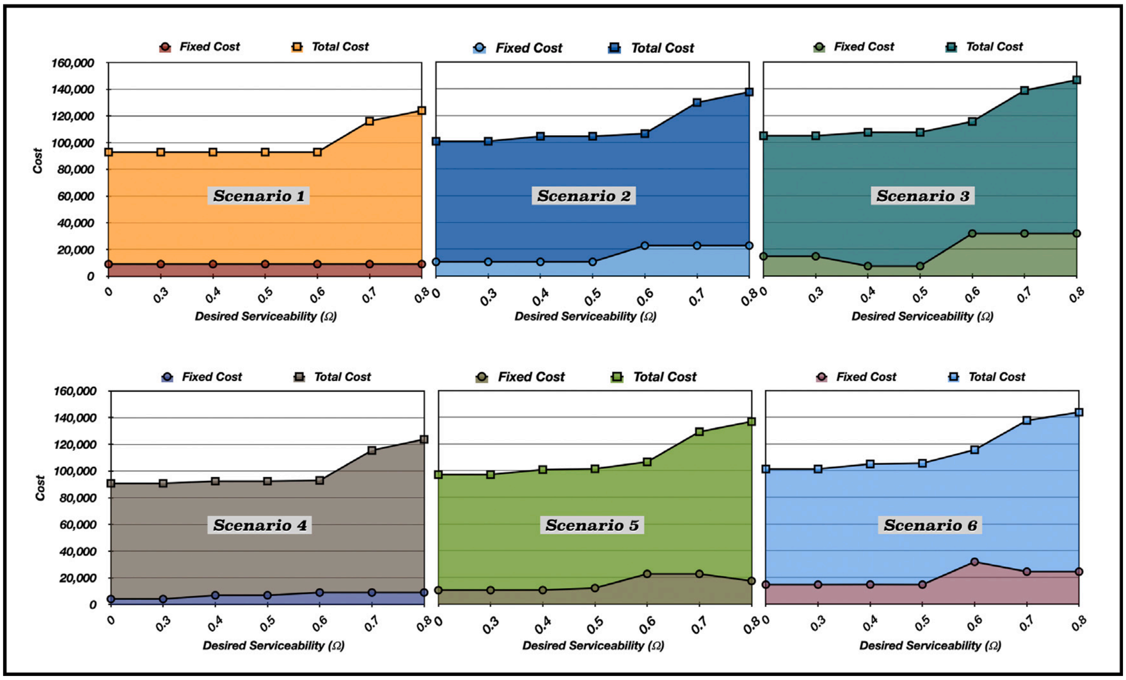

Fig. 5. Sensitivity of the Fixed Cost and Total Cost of the optimal design to increments in the desired service level threshold (Ω) for the six scenarios.

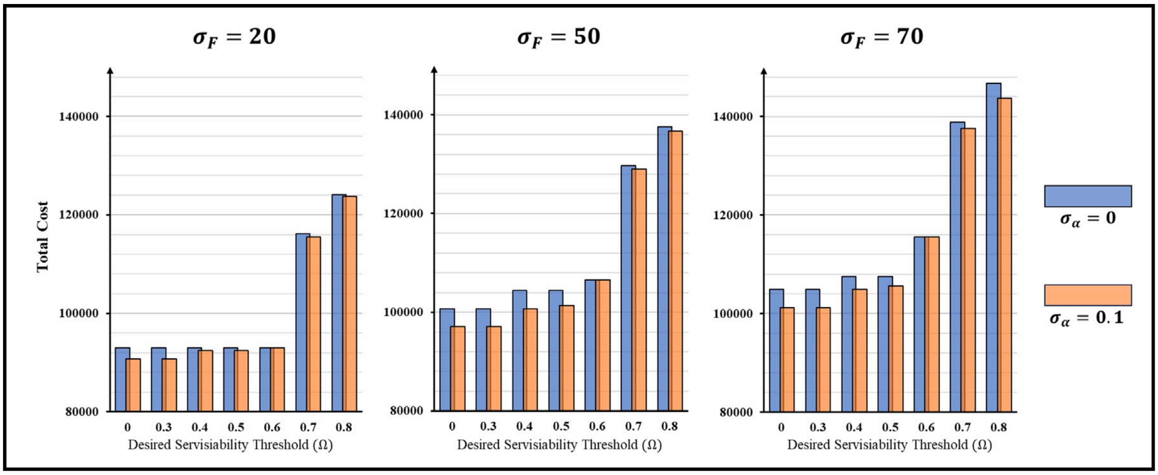

Fig. 6. Sensitivity of the Total Cost of the optimal design to variation in discount factors.

the optimal design in the scenarios with smaller discount factors has significantly less fixed costs in comparison to the respective scenarios from Table 6. However, the overall reduction in the total cost of the system is not as large (check for instance Fig. 6 for $\sigma_F = 20$). That is mainly because, even in Scenarios 3 and 6, the fixed cost of the network accounted for a small proportion of the overall costs of the network. From the reliability perspective, the proposed model performed sufficiently, especially when the desired reliability was significantly high.

To investigate the performance of the proposed model in realizing the desired serviceability levels, Fig. 7 compares the average reliability (serviceability) of the flow between each pair of origin–destination, accompanied by its distribution under all cases of each scenario. Although the model was successful in complying with the defined service level threshold in all scenarios, the range of the reliability values becomes smaller as we pass the knee point of 0.6 for the parameter Ω. Especially, in the last case with the maximum desired reliability, we observe that the difference between the first and third quantile is less than 10%. In general, despite some slight changes in the distribution of the optimal reliability from one scenario to the neighbor one, it does not seem to be significantly sensitive to the fixed establishment cost. The only visible fluctuation of the reliability average is when we transit

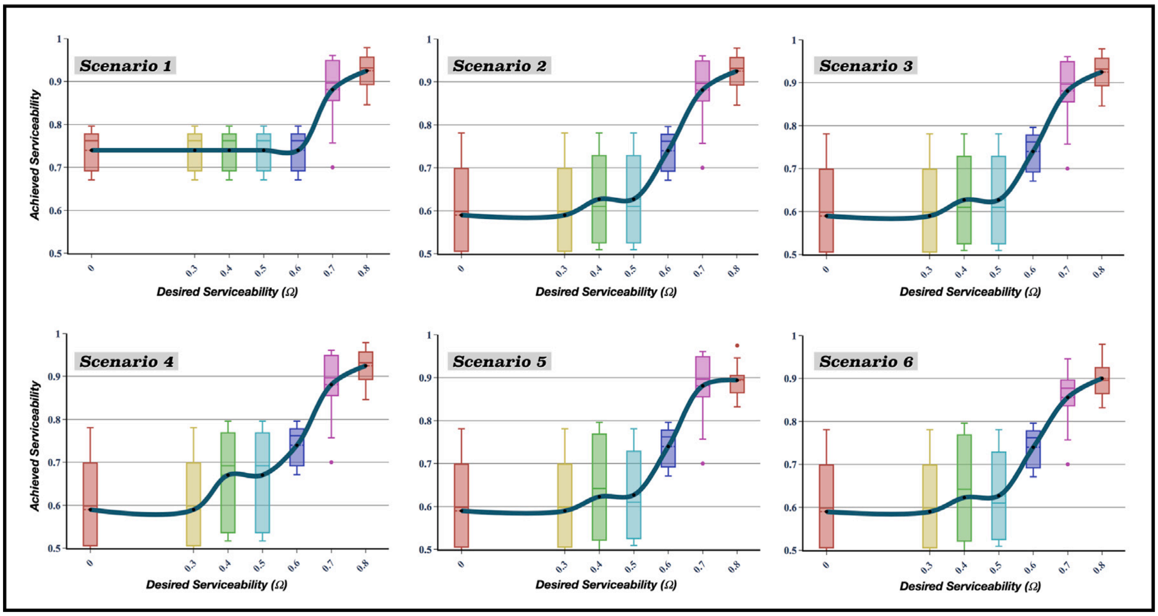

Fig. 7. The achieved reliability (y-axis) in the optimal design vs the desired service level threshold (x-axis), i.e., Ω (solid line represents mean value).

from $\sigma_F = 20$ to $\sigma_F = 50$ in Scenarios 1 to 2 and this decrement in the reliability is limited to Ω values before the aforementioned knee point.

For further analysis, we provide the following graph (Fig. 8) for the total discount in the optimal solution of each scenario and compare the effect of changes in the fixed cost, reliability threshold, and discount factor on the overall performance of the proposed model. Fig. 8 unveils a clear distinction between the first group of scenarios in Table 6 and those in Table 7. In fact, when the discount factor was reduced, the final solution experienced more consolidation to take advantage of the more considerable discounts. Generally speaking, the figure suggests that in order to benefit from the discount in the LTL network, the discount factor for them must be low enough to compete with the other options available in the LTL-HLP. It is seen that the fixed cost of the establishment must also be significant (here, $\sigma_F \geq 50$) to avoid excessive hub establishment.

Here, we see a more noticeable effect of the previously observed knee point on the discounts accumulated by the system. As mentioned earlier, this change in the model behavior shows that on this level of serviceability, the model can no longer satisfy the desired serviceability using the existing number of hubs, and thus sacrifices the discounts and flow consolidation by establishing more hubs. However, it still does not need to force rerouting to the most reliable hubs as the desired reliability is not high yet. This leads to having the flow level in the network fall below the minimum required amount to qualify for the discounts. In other words, at this point, the network is completely impartial to the discount percentage offered (i.e., α_e), thus there is no difference between the defined scenarios, so all achieve no discounts (see point 0.6 for all lines in Fig. 8). As the desired level of reliability is increased to 70% and 80%, the consolidation is financially reasonable again, and the system starts shifting towards configurations with more significant discount accumulation levels. As a future work, it seems to be interesting to investigate the possibility of precise mathematical prediction of this knee point.

The results in Tables 6–7 and the provided analyses support the functionality of the proposed model in achieving the goal of balancing the variable and fixed costs while minimizing the total cost of the network. The model has also completely adapted itself to the various levels of vulnerability in network links to maintain a steady level of serviceability. On the other hand, the model proposed in this study has the ultimate freedom in choosing backup hubs and even deciding on whether to consolidate the flow for LTL discounts. Therefore, it could choose to stay on the no-backup scheme for all parameter settings if the backup strategy was not more cost-efficient. But, we see that under elevated levels of desired reliability, the optimal solution involved backup hubs in all six scenarios. This can prove the superiority of the current approach to the pure hub location problem with no backup. We also observed that the LTL discount system has not been met by the model in many cases, and it has opted out of this cost reduction scheme in favor of other interesting options. This is evidence of the superiority of the proposed method to the pure LTL network design. However, the last two cases of Scenario 6 proved the necessity of considering discount factors, backup hubs, and flow consolidation in only two hubs, simultaneously. The proposed approach is graphically summarized in Fig. 9.

4.2. Cost-resiliency trade-off and managerial insights

In this subsection, we explore the feasibility and benefits of the proposed resilient approach against the traditional approach in which reliability is not a factor in decision-making. For this purpose, we summarize the results of the six scenarios from another

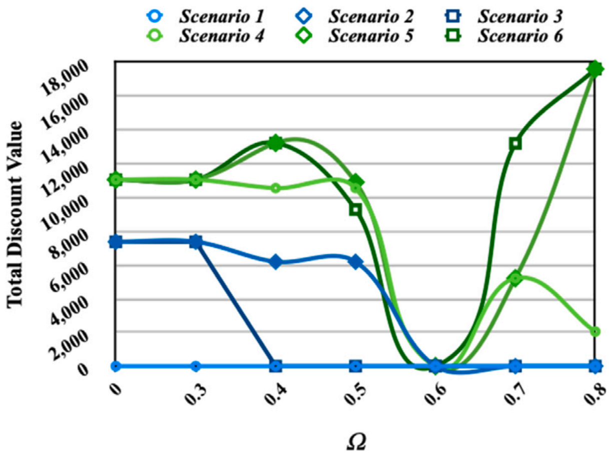

Fig. 8. Performance of the model in achieving discounts under different scenarios.

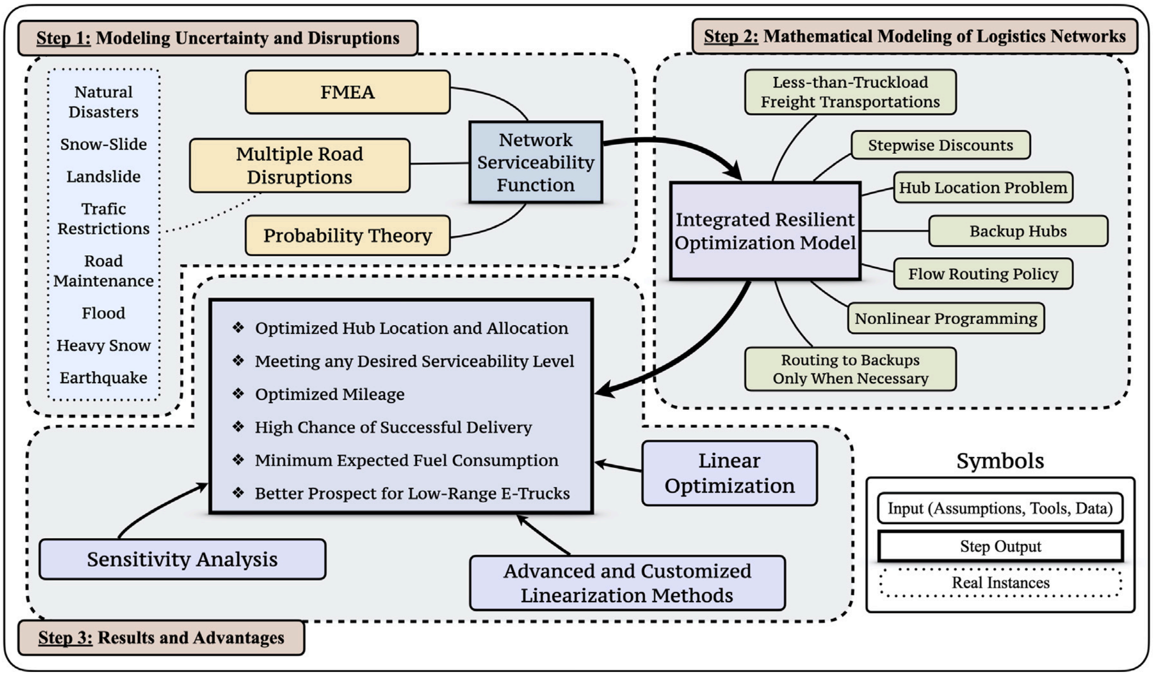

Fig. 9. A schematic view of the steps of the proposed framework.

angle considering only the case in which no reliability requirement is imposed and the last case in each scenario where Ω is set to the highest value (i.e., 0.8). Table 8 compares the reliability range achieved by the traditional approach with the corresponding values from the resilient case while Table 9 contrasts the associated costs.

In Table 8, the lower bound of the reliability represents the minimum level of serviceability that can be guaranteed by the logistics system. For example, when the range is [0.352, 0.781] for the traditional policy, the company is likely to deliver at least 35.2% of their shipments successfully on-time under the considered vulnerabilities in the road conditions. The reliability shifts reported in the table indicate that by applying the proposed modeling process, policymakers can achieve a drastic raise of around 50% in their guaranteed successful on-time delivery. When compared to the original value, this shows a considerable relative improvement of over 140%. Moreover, the cost comparison reported in Table 9 shows that this shift in resiliency only results in up to 42% increase in the overall cost. Even when a very low cost of hub establishment is accompanied by uninteresting discount rates (e.g., Scenario 1), the proposed resilient approach still brings about a very significant improvement in serviceability (over 26%). This is because, in this particular scenario, the maximum possible number of hubs has already been established due to the low establishment cost. Therefore, the fixed cost of the system remains unchanged, and the improvement is attributed solely to more efficient management.

Table 8
Reliability comparison between the resilient model and its traditional counterpart.

Scenario	Reliability range		Amount of change in Min | Max Reliability	Relative Improvement (%)
	Traditional	Resilient		
1	[**0.671**, 0.796]	[**0.846**, 0.979]	**0.175** | 0.183	**26.08** | 22.99
2	[**0.352**, 0.781]	[**0.846**, 0.979]	**0.494** | 0.198	**140.34** | 25.35
3	[**0.352**, 0.781]	[**0.846**, 0.979]	**0.494** | 0.198	**140.34** | 25.35
4	[**0.352**, 0.781]	[**0.846**, 0.979]	**0.494** | 0.198	**140.34** | 25.35
5	[**0.352**, 0.781]	[**0.832**, 0.980]	**0.480** | 0.199	**136.36** | 25.48
6	[**0.352**, 0.781]	[**0.832**, 0.980]	**0.480** | 0.199	**136.36** | 25.48

Table 9
Cost comparison between the resilient model and its traditional counterpart.

Scen.	Traditional			Resilient			Cost Increment (%)		
	Fixed	Variable	Total	Fixed	Variable	Total	Fixed	Variable	Total
1	9049.27	83897.28	**92946.55**	9049.27	115011.13	**124060.40**	0.0	37.1	**33.5**
2	10444.49	90281.35	**100725.84**	22623.18	115011.13	**137634.30**	116.6	27.4	**36.6**
3	14622.29	90281.35	**104903.64**	31672.45	115011.13	**146683.57**	116.6	27.4	**39.8**
4	4177.80	86594.98	**90772.78**	9049.27	114711.48	**123760.75**	116.6	32.5	**36.3**
5	10444.49	86594.98	**97039.47**	17360.60	119375.80	**136736.41**	66.2	37.9	**40.9**
6	14622.29	86594.98	**101217.27**	24304.85	119375.80	**143680.65**	66.2	37.9	**42.0**

As a further advantage, considering the scenario definitions alongside these findings indicates that the aforementioned modifications can be consistently archived notwithstanding potential variations in the fixed establishment costs of the hubs (σ_F) or adjustments to the LTL system's discount levels (i.e., σ_α). This feature inherently enhances the resiliency of the proposed approach, offering policymakers increased confidence when switching to using it. All combined, the noted characteristics of the suggested approach have the potential to revolutionize the competitive logistics market, particularly if rivals start placing a higher priority on timely delivery. For instance, many companies in the urban delivery industry focus on guaranteed successful delivery in the promised time. When introducing its services and products, Saia Inc., a major player in the LTL freight industry in North America, draws customers' attention to its successful delivery rate of over 80% (Saia Inc., 2024). From the competitors' viewpoint, the maintenance of a high reliability index is challenging and costly, especially considering vulnerabilities in road conditions and disruptions. Our results reveal that entering such a serviceability competition will be more affordable by substituting the traditional approach with the proposed one, enabling the achievement of any desired reliability level at the lowest possible cost.

Digging deeper into the reason behind the cost increments after applying the new approach, we notice that the base model lacked a penalty for unsuccessful delivery. In other words, the missed shipment would be overlooked without any financial consequences. This seems to have virtually kept the variable cost lower than the resilient version. Thus, if policymakers consider the penalties and consequences of missed shipments in their systems, they might even see cost reductions after switching to the resilient approach. Penalties imposed on a company greatly depend on the market it operates in. For instance, in a very competitive market, using the traditional approach and failing to deliver a small portion of the shipments (e.g., 30%) might lead to losing the customers — let alone around 70% as in the traditional results of Scenarios 2–6.

Furthermore, even in a single company, the mentioned penalty might be significantly high for specific sets of O–Ds while being negligible for others. The estimation of penalty requires quantifying many factors including but not limited to the loyalty of the customers, the direct penalty in the contracts, the effect of competitors in the market, customers' chance of finding a new service provider, and reputation cost. Consequently, we believe that this type of penalty has to be considered on a case-by-case basis, thus in this study, only the plain cost is reported with no penalties imposed. A great extension to this paper can be a case study focusing on deriving and quantifying these penalties and exploring their effects on the decision-making process.

5. Conclusions

In this paper, we studied a practical integration of the well-known hub location problem with truck-based freight logistics networks. Road availability and route-related disruptions are other concerns that are addressed in the current study. One advantage of the LTL is its discount factor that banks on the economies of scale of the inter-hub transportation. Combining such a disposition with the LTL scheme expands these benefits to the shipment of small loads as well. However, with the disruptions caused by unstable road conditions in mind, the overall service level may suffer from significant fluctuations unless a backup plan is considered. Thus, our mathematical model now includes the option to designate a backup hub for each origin or destination node. This backup hub can be utilized in the event that the primary route is unavailable. In order to calculate the overall reliability of the network after the backup assignment, we explored all possible failure modes and their corresponding effects on the overall service level. A general closed form for the serviceability of the HLP network during multiple link disruptions was introduced that is substantially more practical and realistic compared to other approaches (e.g., chance constraint). Eventually, an integrated mathematical model is presented with the objective of minimizing the total cost of the system, which satisfies a service level threshold.

The proposed model inherits its complexity from both hub location problems and the LTL models. In order to mitigate this complexity, we presented a fully linear version by proposing advanced linearization methods. Results of the suggested linearization approach proved its distinction over alternative techniques in terms of speed, solution quality, and consistency in achieving the global optima. The new model was then investigated through a series of benchmark scenarios. The numerical results reported in this paper showed the superiority of the proposed integrated approach over its counterparts. It was also shown that the model successfully realized the desired service level in all scenarios even when it was set as high as 80%. This, by itself, manifests a great application potential and attractiveness of the current approach for practical usage. The sensitivity analysis provided in this study also suggests that the backup assignment is crucial for such systems if we target attaining a network with reliability levels greater than or equal to 70%. Trade-offs between the system cost and resiliency levels show that the new approach can help newcomers in the urban delivery industry compete more easily with existing players. Existing companies, on the other hand, can utilize its features to enhance their customer satisfaction and market share at an affordable cost.

Based on the proposed framework, in order to implement this approach in real cases, decision-makers should acquire data about the linking roads between the cities of their network coverage. It is worth noting that this is an overlooked link in the literature, and any attempt to propose structured frameworks for collecting such reliability data can be valuable for putting this strategy – as well as other future resilient approaches of a similar nature – into practice. The first step of the framework is concluded by applying the suggested failure mode and effect analysis technique and deriving the system's service level as a function of the decision variables. Given that serviceability is a key performance index of many systems, even if managers decide not to move on to the subsequent mathematical phases, this function can still be highly helpful in assisting them in making better-informed empirical decisions to achieve higher resiliency for their systems. As a second step, we suggest framing the discount policies of the market in a stepwise format. This can then be fed into a mathematical model (similar to the one in this study) that replicates the desired and environmentally fixed characteristics of the company. Once this stage is reached, gaining a fairly resilient system design with all the mentioned benefits is very straightforward using the investigated solution methods.

Given the promising results reported in this study, a possible extension may involve case studies in the logistics industry and further analysis of practical data sets, especially in low-emission freight transportation networks. When looking at the current study solely from the perspective of a reliable hub location problem, the proposed approach with road unavailability is far more practical than the prevalent viewpoint that considered hub unavailability. Our new rerouting policy avoids unnecessary backup route usage. Hypothetically, the main routes are often shorter than the backups, thus this feature of the proposed approach may contribute towards better implementation of battery or fuel-cell operated green trucks that suffer from a limited mileage per single charge. Furthermore, applying the proposed findings on a hybrid intermodal rail-road network and studying the optimal network policies for that case are other interesting possible extensions of this paper for future works.

CRediT authorship contribution statement

Ahmad Attar: Writing – review & editing, Writing – original draft, Visualization, Validation, Software, Resources, Project administration, Methodology, Investigation, Formal analysis, Data curation, Conceptualization. **Chandra Ade Irawan:** Writing – review & editing, Validation, Supervision, Conceptualization. **Ali Akbar Akbari:** Writing – original draft, Supervision, Resources, Project administration, Data curation, Conceptualization. **Shuya Zhong:** Writing – review & editing, Supervision, Conceptualization. **Martino Luis:** Writing – review & editing, Supervision, Conceptualization.

Declaration of competing interest

The authors declare that they have no known competing financial interests or personal relationships that could have appeared to influence the work reported in this paper.

Appendix. Linearization verification

In order to verify the validity of the proposed linearization methods, we selected some of the scenarios presented in Table 6 and solved them in three different ways, i.e., using (i) our proposed linearized version of Ro-LTL-HLP, (ii) the original nonlinear Ro-LTL-HLP via an Exact method, and (iii) the original nonlinear Ro-LTL-HLP via a meta-heuristic algorithm. The exact solvers used in this comparison are the well-known GAMS/CPLEX and BARON for linear and nonlinear models, respectively. For the nonlinear exact solver, however, because of the initial experiments reported in Section 4.1, we extended the maximum allowable time of each run to 72 h. On the other hand, the Genetic Algorithm (GA) was chosen as a representative of the metaheuristic category due to its numerous successful applications in logistics problems (Min, 2015; Azizi et al., 2016; Jauhar and Pant, 2016). The results of these methods for each of the selected scenarios are reported in Table A.1. To have a fair time comparison between the methods, time measurements reported in this section are all done on a Linux-operated computer with a 4-core CPU (2.5 Gigahertz) and 16 GB of RAM.

In Table A.1, we can observe that the proposed linear model using CPLEX successfully found the global optimal solution in all scenarios. Looking at the results of the original nonlinear model, BARON failed to obtain the solutions within a maximum computational time of 72 h. This is a considerable drawback for this MINLP method as it never assured us of global optimality. We suspect that this is mainly because of the very large number of possible combinations for the decision variables. Based on the gap values between BARON and the global optima, its only positive side is that, in some cases, its local optima was in fact the global

Table A.1
Performance comparison between the proposed linearization method and other available options (sample scenarios from Table 6).

Scenario Spec.		Ro-LTL-HLP Model + Proposed Linearization (Exact Method — GAMS/CPLEX Solver)			Ro-LTL-HLP Model (MINLP)							
					Exact Method — BARON				Metaheuristic — Genetic Algorithm			
σ_F	Ω	Total cost	CPUtime(s)	Termination [Sol. Type]	Total cost	CPU Time(s)	Termination [Sol. Type]	Gap	Total cost best [worst]	Avg.CPU time(s)	Termination	Gap best [worst]
20	0.3	**92946.55**	13.49	Normal [**Global**]	92946.55	259217.16	Time Limit [Local]	0	92946.55 [92946.55]	142.63	Iter. Limit	0 [0]
20	0.7	**116168.97**	19.31	Normal [**Global**]	119284.63	265748.27	Time Limit [Local]	3115.7	116168.97 [116168.97]	105.91	Iter. Limit	0 [0]
50	0.6	**106520.46**	23.18	Normal [**Global**]	106520.46	259219.03	Time Limit [Local]	0	106520.46 [109332.2]	120.92	Iter. Limit	0 [2811.74]
50	0.4	**104458.05**	26.87	Normal [**Global**]	106520.46	259225.79	Time Limit [Local]	2062.41	104458.05 [106520.46]	106.78	Iter. Limit	0 [2062.41]
70	0.5	**107457.01**	11.84	Normal [**Global**]	115569.73	259227.77	Time Limit [Local]	8112.72	107457.01 [114138.42]	108.87	Iter. Limit	0 [6681.41]
70	0.8	**146683.57**	181.17	Normal [**Global**]	146683.57	260080.26	Time Limit [Local]	0	146683.57 [146683.57]	105.03	Iter. Limit	0 [0]

solution. We expect this solver to converge in a few more days. Nevertheless, we did not test this theory (i.e., very long run) any further as it does not seem to contribute to our current research.

The genetic algorithm used in this section is the standard GA for which the population size, crossover rate, and mutation rate were all set experimentally to 50, 75%, and 30%, respectively. Furthermore, our experiments showed acceptable results when the maximum number of iterations was set to 100. The algorithm is coded using Python programming language and all the runs are done on a computer with the abovementioned specifications. For further information about the procedure of GA and its parameters, one may refer to Min (2015), Azizi et al. (2016), and Jauhar and Pant (2016). Due to the random nature of the search in GA, we ran the algorithm 30 times and reported the best and worst solutions in Table A.1 accompanied by the average time consumed per run.

It is revealed that GA successfully found the optimal solution in all scenarios as the gap between the global solution and the best solution found in the 30 runs is 0 for all explored settings. Still, the worst solution occasionally had a significant gap from the global optima. This indicates that even though, in some cases, the average time consumed in each run of GA is slightly shorter than CPLEX (e.g., last scenario in Table A.1), GA will require a sample of multiple runs. As a result, the actual computational time for assuring global optimality in GA is multiple times the reported average, whereas CPLEX requires a single run only. This weakness was also reported by other studies for GA family and other metaheuristic algorithms (Attar et al., 2015, 2017, 2023b). Therefore, we can conclude that the linearization method can be more time-efficient than the metaheuristic approach.

By summarizing the above observations, not only can we conclude the validity of the proposed exact linearization approach, but also confirm its significant superiority from multiple aspects including the overall speed, quality of solution, and consistency in achieving the global optima.

References

Adler, N., Njoya, E.T., Volta, N., 2018. The multi-airline *p*-hub median problem applied to the african aviation market. Transp. Res. Part A: Policy Pract. 107, 187–202.

Alumur, S.A., Campbell, J.F., Contreras, I., Kara, B.Y., Marianov, V., O'Kelly, M.E., 2021. Perspectives on modeling hub location problems. European J. Oper. Res. 291 (1), 1–17.

Alumur, S., Kara, B.Y., 2008. Network hub location problems: The state of the art. European J. Oper. Res. 190 (1), 1–21.

An, Y., Zhang, Y., Zeng, B., 2015. The reliable hub-and-spoke design problem: Models and algorithms. Transp. Res. B 77, 103–122.

Attar, A., Jin, Y., Luis, M., Zhong, S., Sucala, V.I., 2023a. Simulation-based analyses and improvements of the smart line management system in canned beverage industry: A case study in europe. In: Proceedings of the Winter Simulation Conference. IEEE, pp. 2124–2135.

Attar, A., Raissi, S., Khalili-Damghani, K., 2015. Multi-objective reliability-redundancy allocation for non-exponential multi-state repairable components. In: 11th International Conference of Industrial Engineering - IIEC2015. pp. 1–8.

Attar, A., Raissi, S., Khalili-Damghani, K., 2017. A simulation-based optimization approach for free distributed repairable multi-state availability-redundancy allocation problems. Reliab. Eng. Syst. Saf. 157, 177–191.

Attar, A., Raissi, S., Tohidi, H., Feizollahi, M.J., 2023b. A novel perspective on reliable system design with erlang failures and realistic constraints for incomplete switching mechanisms. IEEE Access 11, 51900–51914.

Aykin, T., 1988. On the location of hub facilities. Transp. Sci. 22 (2), 155–157.

Aykin, T., 1994. Lagrangian relaxation based approaches to capacitated hub-and-spoke network design problem. European J. Oper. Res. 79 (3), 501–523.

Aykin, T., 1995a. The hub location and routing problem. European J. Oper. Res. 83 (1), 200–219.

Aykin, T., 1995b. Networking policies for hub-and-spoke systems with application to the air transportation system. Transp. Sci. 29 (3), 201–221.

Azizi, N., Chauhan, S., Salhi, S., Vidyarthi, N., 2016. The impact of hub failure in hub-and-spoke networks: Mathematical formulations and solution techniques. Comput. Oper. Res. 65, 174–188.

Azizi, N., García, S., Irawan, C.A., 2022. Discrete location problems with uncertainty. In: The Palgrave Handbook of Operations Research. Springer, pp. 43–71.

Azizi, N., Salhi, S., 2022. Reliable hub-and-spoke systems with multiple capacity levels and flow dependent discount factor. European J. Oper. Res. 298 (3), 834–854.

Barabadi, A., Barabady, J., Markeset, T., 2014. Application of reliability models with covariates in spare part prediction and optimization – A case study. Reliab. Eng. Syst. Saf. 123, 1–7.

Barahimi, P., Vergara, H.A., 2020. Reliable p-hub network design under multiple disruptions. Netw. Spat. Econ. 20 (1), 301–327.

Bíl, M., Vodák, R., Kubeček, J., Bílová, M., Sedoník, J., 2015. Evaluating road network damage caused by natural disasters in the czech Republic between 1997 and 2010. Transp. Res. Part A: Policy Pract. 80, 90–103.

Bryan, D., 1998. Extensions to the hub location problem: Formulations and numerical examples. Geogr. Anal. 30 (4), 315–330.

Buccheri, G., Livieri, G., Pirino, D., Pollastri, A., 2020. A closed-form formula characterization of the epps effect. Quant. Finance 20 (2), 243–254.

Carlson, C.S., 2014. Understanding and applying the fundamentals of FMEAs. In: Annual Reliability and Maintainability Symposium, vol. 10, pp. 1–35.

Chang, C.-T., Chang, C.-C., 2000. A linearization method for mixed 0–1 polynomial programs. Comput. Oper. Res. 27 (10), 1005–1016.

Chen, S., Yan, Y., Song, H., 2010. Optimal logistics hubs locations on the multimodal transportation network. In: ICLEM 2010: Logistics for Sustained Economic Development: Infrastructure, Information, Integration. pp. 2850–2855.

Collin-Dufresne, P., Harding, J.P., 1999. A closed form formula for valuing mortgages. J. Real Estate Finance Econ. 19, 133–146.

Contreras, I., O'Kelly, M., 2019. Hub location problems. In: Location Science. Springer, pp. 327–363.

Cunha, C.B., Silva, M.R., 2007. A genetic algorithm for the problem of configuring a hub-and-spoke network for a LTL trucking company in Brazil. European J. Oper. Res. 179 (3), 747–758.

Davari, S., Zarandi, M.H.F., Turksen, I.B., 2010. The fuzzy reliable hub location problem. In: 2010 Annual Meeting of the North American Fuzzy Information Processing Society. IEEE, pp. 1–6.

Eydi, A., Nasiri, R., 2019. A P-hub median network design problem with preventive reliability approach for before and after hub failure. Sādhanā 44, 1–18.

Farahani, R.Z., Hekmatfar, M., Arabani, A.B., Nikbakhsh, E., 2013. Hub location problems: A review of models, classification, solution techniques, and applications. Comput. Ind. Eng. 64 (4), 1096–1109.

Ghezavati, V.R., Saidi-Mehrabad, M., 2011. An efficient linearization technique for mixed 0–1 polynomial problem. J. Comput. Appl. Math. 235 (6), 1730–1738.

Hakimi, S.L., 1964. Optimum locations of switching centers and the absolute centers and medians of a graph. Oper. Res. 12 (3), 450–459.

Hernández, S., Unnikrishnan, A., Awale, S.S., 2012. Centralized carrier collaboration multihub location problem for less-than-truckload industry: Hybrid hub-and-spoke network. Transp. Res. Rec. 2269 (1), 20–28.

Jauhar, S.K., Pant, M., 2016. Genetic algorithms in supply chain management: A critical analysis of the literature. Sādhanā 41, 993–1017.

Jenelius, E., Mattsson, L.-G., 2012. Road network vulnerability analysis of area-covering disruptions: A grid-based approach with case study. Transp. Res. Part A: Policy Pract. 46 (5), 746–760.
Kara, B.Y., Tansel, B.C., 2000. On the single-assignment *p*-hub center problem. European J. Oper. Res. 125 (3), 648–655.
Kim, H., O'Kelly, M.E., 2009. Reliable *p*-hub location problems in telecommunication networks. Geogr. Anal. 41 (3), 283–306.
Kudláč, v., Štefancová, V., Majerčák, J., 2017. Using the saaty method and the FMEA method for evaluation of constraints in logistics chain. Procedia Eng. 187, 749–755.
Lin, C.-C., Lee, S.-C., 2010. The competition game on hub network design. Transp. Res. B 44 (4), 618–629.
Lin, C.-C., Lee, S.-C., 2018. Hub network design problem with profit optimization for time-definite LTL freight transportation. Transp. Res. Part E: Logist. Transp. Rev. 114, 104–120.
Martin, J.C., Román, C., 2003. Hub location in the south-atlantic airline market: A spatial competition game. Transp. Res. Part A: Policy Pract. 37 (10), 865–888.
Meier, J.F., Clausen, U., 2018. Solving single allocation hub location problems on euclidean data. Transp. Sci. 52 (5), 1141–1155.
Min, H., 2015. Genetic algorithm for supply chain modelling: basic concepts and applications. Int. J. Serv. Oper. Manag. 22 (2), 143–164.
Mohammadi, M., Jolai, F., Tavakkoli-Moghaddam, R., 2013. Solving a new stochastic multi-mode *p*-hub covering location problem considering risk by a novel multi-objective algorithm. Appl. Math. Model. 37 (24), 10053–10073.
Mohammadi, M., Jula, P., Tavakkoli-Moghaddam, R., 2019. Reliable single-allocation hub location problem with disruptions. Transp. Res. Part E: Logist. Transp. Rev. 123, 90–120.
Mohri, S.S., Thompson, R., 2022. Designing sustainable intermodal freight transportation networks using a controlled rail tariff discounting policy–the Iranian case. Transp. Res. Part A: Policy Pract. 157, 59–77.
Momayezi, F., Chaharsooghi, S.K., Sepehri, M.M., Kashan, A.H., 2021. The capacitated modular single-allocation hub location problem with possibilities of hubs disruptions: modeling and a solution algorithm. Oper. Res. 21 (1), 139–166.
Navarro, J., 2022. Introduction to System Reliability Theory. Springer Nature.
Niknamfar, A.H., Niaki, S.T.A., Niaki, S.A.A., 2017. Opposition-based learning for competitive hub location: A bi-objective biogeography-based optimization algorithm. Knowl.-Based Syst. (ISSN: 0950-7051) 128, 1–19.
Qu, B., Weng, K., 2009. Path relinking approach for multiple allocation hub maximal covering problem. Comput. Math. Appl. 57 (11–12), 1890–1894.
Rostami, B., Kämmerling, N., Buchheim, C., Clausen, U., 2018. Reliable single allocation hub location problem under hub breakdowns. Comput. Oper. Res. 96, 15–29.
Saia Inc., 2024. Saia LTL freight's Products and Services. URL https://saia.com/products-and-services.
Scipioni, A., Saccarola, G., Centazzo, A., Arena, F., 2002. FMEA methodology design, implementation and integration with HACCP system in a food company. Food Control 13 (8), 495–501.
Shahabi, A., Raissi, S., Khalili-Damghani, K., Rafei, M., 2022. An event-driven simulation-optimisation approach to improve the resiliency of operation in a double-track urban rail line. J. Simul. 16 (5), 526–545.
Siskos, P., Moysoglou, Y., 2019. Assessing the impacts of setting CO2 emission targets on truck manufacturers: A model implementation and application for the EU. Transp. Res. Part A: Policy Pract. 125, 123–138.
Takano, K., Arai, M., 2009. A genetic algorithm for the hub-and-spoke problem applied to containerized cargo transport. J. Mar. Sci. Technol. 14, 256–274.
Takebayashi, M., 2018. Managing airport charges under the multiple hub network with high speed rail: Considering capacity and gateway function. Transp. Res. Part A: Policy Pract. 112, 108–123.
Tang, W., Chen, X., Lang, M., Li, S., Liu, Y., Li, W., 2024. Optimization of truck–cargo online matching for the less-than-truck-load logistics hub under real-time demand. Mathematics 12 (5), 755.
Toh, R.S., Higgins, R.G., 1985. The impact of hub and spoke network centralization and route monopoly on domestic airline profitability. Transp. J. 24 (4), 16–27.
Tordecilla, R.D., Juan, A.A., Montoya-Torres, J.R., Quintero-Araujo, C.L., Panadero, J., 2021. Simulation-optimization methods for designing and assessing resilient supply chain networks under uncertainty scenarios: A review. Simul. Model. Pract. Theory 106, 102166.
Tsai, M.-C., 2006. Constructing a logistics tracking system for preventing smuggling risk of transit containers. Transp. Res. Part A: Policy Pract. 40 (6), 526–536.
Wang, Q., Zheng, J., Liu, X., 2023. Reliable liner shipping hub location problem considering hub failure. J. Mar. Sci. Eng. 11 (4), 818.
Yahyaei, M., Bashiri, M., Randall, M., 2019. A model for a reliable single allocation hub network design under massive disruption. Appl. Soft Comput. 82, 105561.
Yang, T.-H., 2009. Stochastic air freight hub location and flight routes planning. Appl. Math. Model. 33 (12), 4424–4430.
Zhang, Q., Yu, H., Li, Z., Zhang, G., Ma, D.T., 2020. Assessing potential likelihood and impacts of landslides on transportation network vulnerability. Transp. Res. Part D: Transp. Environ. 82, 102304.
Zhao, Q., Wu, T., Duan, J., Hong, J., 2024. A novel Bayesian-inference-based method for global sensitivity analysis of system reliability with multiple failure modes. Struct. Saf. 106, 102394.